

AD-A110 981 ROCKWELL INTERNATIONAL CEDAR RAPIDS IA COLLINS TELECOM-ETC F/6 17/2.1
TRANSCIVER MULTIPLEXERS TD-1288()/6RC AND TD-1289()/6RC.(U)
FEB 82 D PENNER, J DEAN DAAB07-77-C-0193
UNCLASSIFIED 523-0769373-00121D-F CECOM-77-0193-F NL

1 OF 1
ADA
10/8

END
DATE
FILMED
03-82
DTIC



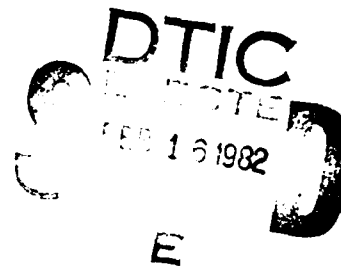
LEVEL II

12

RESEARCH AND DEVELOPMENT TECHNICAL REPORT
CECOM — 77-0193-F

AD A110981
**TRANSCEIVER MULTIPLEXERS
TD-1288()/GRC AND
TD-1289()(V)/GRC**

D. Penner/J. Dean
Rockwell International
Collins ~~Government~~ Telecommunications Products Division
Cedar Rapids, Iowa 52498



Final Report for 1 October 1977 — 30 December 1980

Feb 1982

Distribution Statement

Approved for public release;
distribution unlimited.

Prepared for

Center for Communication Systems
CECOM

US ARMY COMMUNICATIONS - ELECTRONICS COMMAND
FORT MONMOUTH, NEW JERSEY 07703

DTIC FILE COPY

82 02 16 023

NOTICES

Disclaimers

The citation of trade names and names of manufacturers in this report is not to be construed as official Government endorsement or approval of commercial products or services referenced herein.

Disposition

Destroy this report when it is no longer needed. Do not return it to the originator.

SECURITY CLASSIFICATION OF THIS PAGE (When Data Entered)

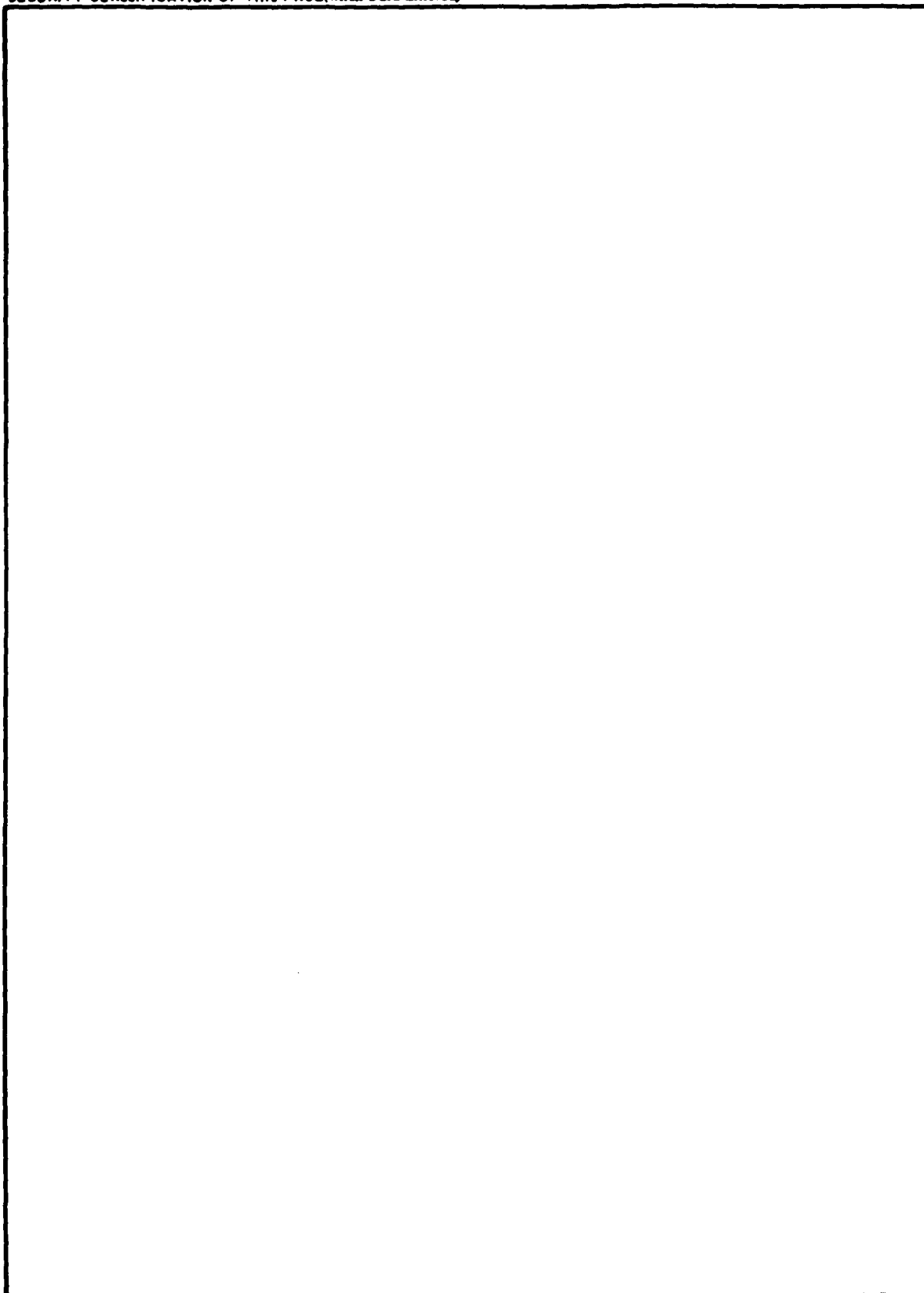
REPORT DOCUMENTATION PAGE		READ INSTRUCTIONS BEFORE COMPLETING FORM
1. REPORT NUMBER CECOM-77-0193-F	2. GOVT ACCESSION NO. AD-A110 981	3. RECIPIENT'S CATALOG NUMBER
4. TITLE (and Subtitle) Transceiver Multiplexers TD-1288()/GRC and TD-1289()/GRC		5. TYPE OF REPORT & PERIOD COVERED G002 Final Report 10/1/77 - 12/30/80
		6. PERFORMING ORG. REPORT NUMBER 523-0769373-00121D
7. AUTHOR(s) D. Penner, J. Dean		8. CONTRACT OR GRANT NUMBER(s) DAAB07-77-C-0193
9. PERFORMING ORGANIZATION NAME AND ADDRESS Rockwell International Collins Government Telecommunications Prods. Div. Cedar Rapids, Iowa 52498		10. PROGRAM ELEMENT, PROJECT, TASK AREA & WORK UNIT NUMBERS 1x4 64701 D488 66 01
11. CONTROLLING OFFICE NAME AND ADDRESS CENCOMS US Army CECOM, DRDCO-COM-RN-1 Fort Monmouth, New Jersey 07703		12. REPORT DATE Feb 1982
		13. NUMBER OF PAGES 67
14. MONITORING AGENCY NAME & ADDRESS (if different from Controlling Office)		15. SECURITY CLASS. (of this report) Unclassified
		15a. DECLASSIFICATION/DOWNGRADING SCHEDULE
16. DISTRIBUTION STATEMENT (of this Report) Approved for Public Release, distribution unlimited.		
17. DISTRIBUTION STATEMENT (of the abstract entered in Block 20, if different from Report)		
18. SUPPLEMENTARY NOTES		
19. KEY WORDS (Continue on reverse side if necessary and identify by block number) Bandpass filters, coupling circuits, filters, Helical Resonator, Matching network, RF tuning capacitors, Transceiver multiplexer. Antenna coupler, Transceiver Multicoupler		
20. ABSTRACT (Continue on reverse side if necessary and identify by block number) This final report summarizes the activity on Contract DAAB07-77-C-0193. It describes a 2-channel and a 5-channel vhf multiplexer developed for use in the 30 MHz to 88 MHz range. The frequency range of a multiplexer developed under a previous contract was extended and a termination unit to replace an unused channel was developed. Ten 2-channel and ten 5-channel multiplexers, six termination units, and seven spare filters were built. Each multiplexer was supplied with a case for protection in transit.		

DD FORM 1473

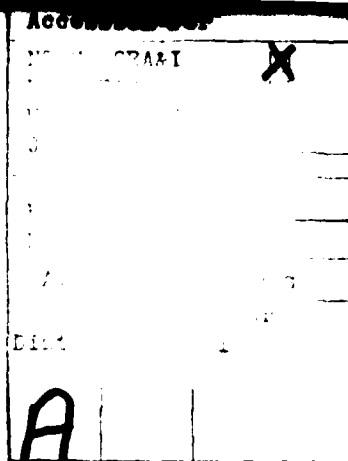
EDITION OF 1 NOV 65 IS OBSOLETE

SECURITY CLASSIFICATION OF THIS PAGE (When Data Entered)

SECURITY CLASSIFICATION OF THIS PAGE(When Data Entered)



SECURITY CLASSIFICATION OF THIS PAGE(When Data Entered)



Page

List of Illustrations

i

List of Illustrations (Cont)

Figure	Page
2-7 Equivalent Circuit of an Off-Channel Branch	2-13
2-8 Equivalent Circuit of an On-Channel Branch	2-14
2-9 Measured Output Terminal Q	2-16
2-10 Helical Resonator Dimensions	2-18
2-11 Norton's First Transformation	2-22
2-12 Reduction of Transformer to Final Form	2-23
2-13 Broadband Transformer Calculations	2-25
2-14 Broadband Transformer, Final Values	2-26
2-15 Matching Section Element Determination	2-28
2-16 Final Coupler Configuration	2-29
2-17 Measured Input Terminal Q	2-30
2-18 Measured Coupling Coefficient	2-31
2-19 Filter, Simplified Block Diagram	2-32
2-20 Directional Coupler, Simplified Schematic	2-32
2-21 90° Discriminator, Simplified Schematic	2-33
3-1 5-Channel Multiplexer (TD-1289()/V1/GRC)	3-2
3-2 4-Channel Multiplexer (TD-1289()/V2/GRC)	3-2
3-3 3-Channel Multiplexer (TD-1289()/V3/GRC)	3-3
3-4 2-Channel Multiplexer (TD-1288()/GRC)	3-3
3-5 2-Channel Coupler (CU-2266()/GRC)	3-3
3-6 5-Channel Coupler (CU-2267()/GRC)	3-4
3-7 Termination Unit (MX-10080()/GRC)	3-4
3-8 Termination Unit With Cover Removed (MX-10080()/GRC)	3-4
3-9 Bandpass Filter, Exploded View (F-1482()/GRC)....	3-5
3-10 Bandpass Filter, Rear View (F-1482()/GRC).....	3-5
3-11 Transit Case-5-Channel Multiplexer (CY-7776()/GRC)	3-6
3-12 Transit Case-2-Channel Multiplexer (CY-7775()/GRC)	3-6
3-13 Measured Insertion Loss for the TD-1289()/V1/ GRC 5-Channel Multiplexer	3-6
3-14 Measured Transceiver Port to Transceiver Port Attenuation	3-9
3-15 Measured VSWR at Transceiver Input	3-10
3-16 Intermodulation Levels of Three Filter Combina- tions vs Frequency for a 5-Channel Multiplexer with Improved Variable Capacitors (TD-1289() (V)1/GRC Unit 4A)	3-11
3-17 Bandpass Filter, Exploded View (F-1482()/GRC)...	3-12
3-18 Bandpass Filter, Rear View (F-1482()/GRC)	3-12
3-19 Outline Drawing, Bandpass Filter (F-1482()/GRC)	3-13

List of Illustrations (Cont)

Figure	Page
3-20 5-Channel Coupler, Interior View (CU-2267()/GRC)	3-13
3-21 2-Channel Coupler, Interior View (CU-2266()/GRC)	3-14
3-22 Outline Drawing, 2-Channel Multiplexer (TD-1288()/GRC)	3-15
3-23 Outline Drawing, 5-Channel Multiplexer (TD-1289()(V)1/GRC)	3-16
3-24 Schematic, Bandpass Filter (F-1482()/GRC)	3-17
3-25 Schematic, Power Discriminator (Directional Coupler)	3-18
3-26 Schematic, Phasing Discriminator	3-18
3-27 Schematic, 2-Channel Coupler (CU-2266()/GRC) ...	3-19
3-28 Schematic, 5-Channel Coupler (CU-2267()/GRC) ...	3-19

List of Tables

Table	Page
1-1 Equipment Nomenclature	1-2
2-1 Terminal Q Versus Number of Resonators	2-8
2-2 S-Dimension Versus Number of Resonators for a Total Filter Volume of $54.675 \ln^3$	2-10
2-3 Resonator Unloaded Q for a $54.675\text{-}\ln^3$ Filter	2-10
2-4 Insertion Loss Versus the Number of Resonators for a Minimum Loss Filter of $54.675 \ln^3$, Having 40 dB of Attenuation 5 Percent From the Operating Frequency	2-11
2-5 Optimum Parameters for Output Coupling Circuit ...	2-15
2-6 Resonator Measured Unloaded Q	2-21
3-1 Tuning Procedure for VHF Multiplexer	3-20

This report describes the design, fabrication, and test of both the TD-1288()/GRC, 2-channel transceiver multiplexer, and the TD-1289()(V)/GRC, 5-channel transceiver multiplexer. Respectively, these multiplexers permit simultaneous use of two or five transceivers on a single broadband antenna over the frequency range of 30 MHz to 88 MHz. Both versions of multiplexers consist of (two or five) identical, manually tuned, 3-pole filter modules mounted on a base. This base contains a 2- or 5-channel combining/matching network that allows the rf output terminals of the individual filter modules to be connected together and operated on a common antenna. US Army Electronics Command Development Specification, EL-CP0192-0001A dated 22 March 1977, describes the physical, performance, and environmental characteristics and capabilities of the multiplexers.

Although the contract required the development of a 2-channel multiplexer, a 5-channel multiplexer, spare filters, and termination units, the design approach allows the basic filters to be used in a variety of multiplexer bases that can accommodate from 2 to 10 filters, thereby forming multiplexers with 2 to 10 channels.

The filter, for each channel of the multiplexer, is a minimum-loss 3-resonator filter. Each resonator of the filter consists of a capacitively tuned helical resonator. Fixed coupling structures are used throughout the filter. This provides a practical, simple, easily reproducible design. The internal aperture couplings provide a constant coefficient of coupling as the filter is tuned over the operating frequency range, thus providing a constant percentage bandwidth characteristic. Input and output couplings allow a nearly constant terminal Q as required for a constant percentage bandwidth filter.

The input coupling employs a fixed series inductor tapped into the input resonator. This form of coupling provides good coupling characteristics along with minimum resonator frequency shift. The output coupling is designed such that up to 10 filters may be connected to form a multiplexer. This output coupling in conjunction with the interconnecting lines and a broadband matching network provides the desired multiplexer performance. The matching network is designed to be broadband such that no adjustment, tuning, or band switching is required, as the frequency of the channels is changed.

Overall measured performance of the deliverable hardware is good. No tuning interaction between the channels has been observed for frequency spacings greater than five percent. A summary of the measured performance is presented in this report. Details of the Engineering Design Test (qualification test) have been presented in the Engineering Accomplishment Report/Evaluation Report as part of this contract.

Detailed schematics of the filter and matching networks are presented. Constructional details of the helical resonators, apertures, couplings, and matching networks are included.

Table 1-1 details the nomenclature assignments for the various pieces of equipment and states the quantities delivered as unique items under this contract. Figure 1-1 describes the configuration of modules for the 5-channel, 4-channel, 3-channel and 2-channel multiplexers.

Table 1-1. Equipment Nomenclature.

QUANTITY BUILT	NOMENCLATURE	DESCRIPTION
10	TD-1289() (V)1/GRC	5-channel multiplexer
None	TD-1289() (V)2/GRC	4-channel multiplexer
None	TD-1289() (V)3/GRC	3-channel multiplexer
10	TD-1288()/GRC	2-channel multiplexer
77*	F-1482()/GRC	Bandpass filter
10**	CU-2267()/GRC	5-channel coupler
10***	CU-2266()/GRC	2-channel coupler
6	MX-10080()/GRC	Termination unit
10	CY-7775()/GRC	2-channel multiplexer transit case
10	CY-7776()/GRC	5-channel multiplexer transit case

*50 F-1482()/GRC filters are a part of the 10 TD-1289() (V)1/GRC 5-Channel Multiplexers.

20 F-1482()/GRC filters are a part of the 10 TD-1288()/GRC 2-Channel Multiplexers.

7 F-1482()/GRC filters are spares.

**All 10 CU-2267()/GRC 5-Channel Couplers are a part of the TD-1289() (V)1/GRC 5-Channel Multiplexers.

***All 10 CU-2266()/GRC 2-Channel Couplers are a part of the TD-1288()/GRC 2-Channel Multiplexers.

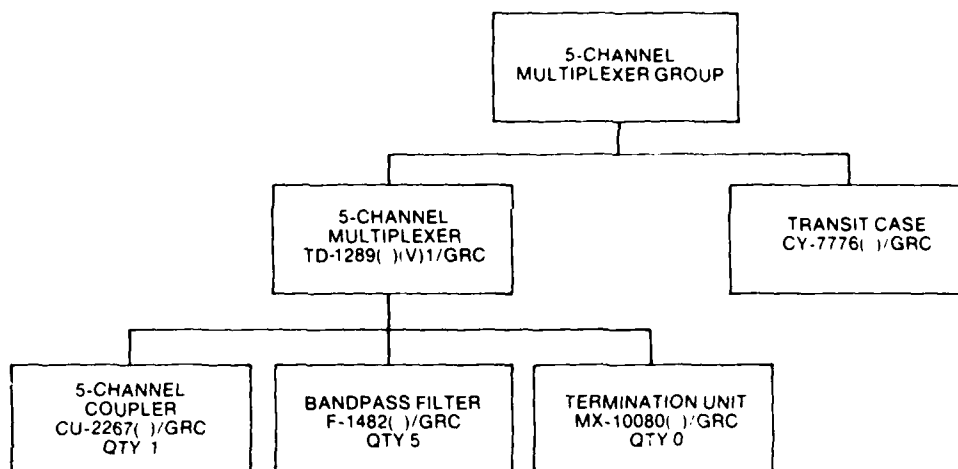


Figure 1-1.a VHF Multiplexer Family Tree.

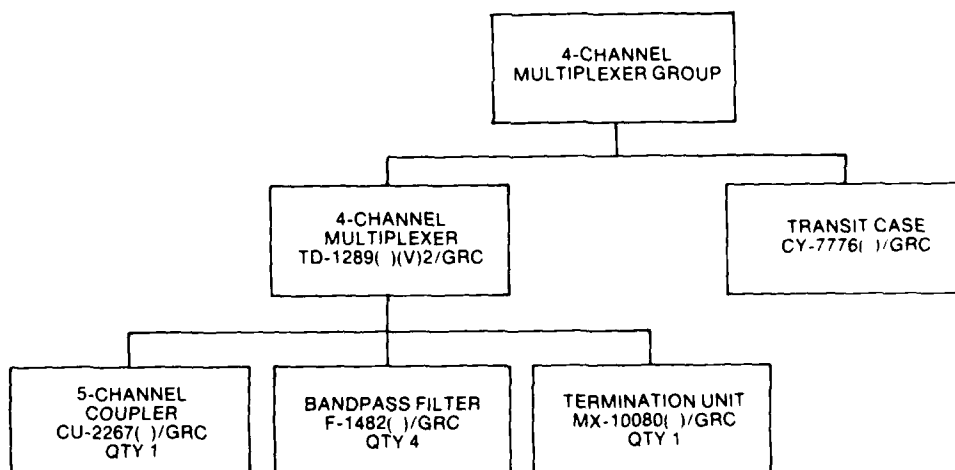


Figure 1-1.b VHF Multiplexer Family Tree.

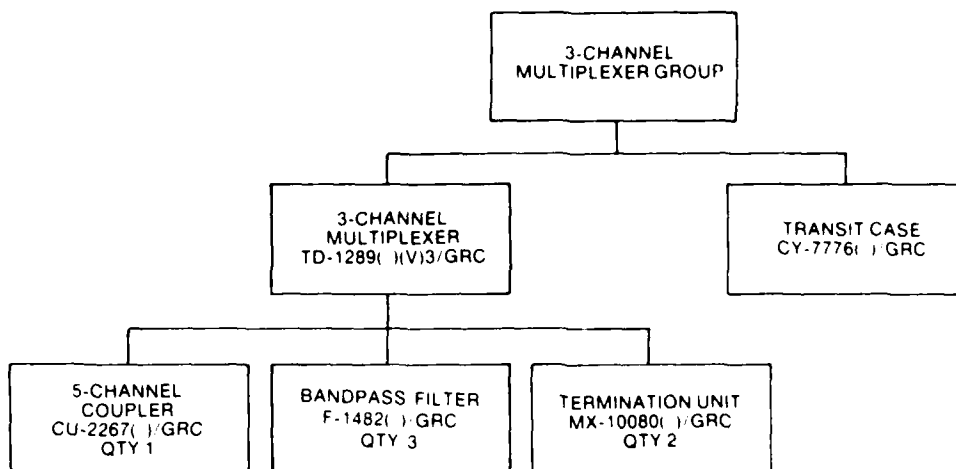


Figure 1-1.c VHF Multiplexer Family Tree.

Although the 5-channel multiplexer would perform satisfactorily with three termination units and two bandpass filters or four termination units and one bandpass filter, these are not approved US Army configurations and they do not have assigned nomenclature.

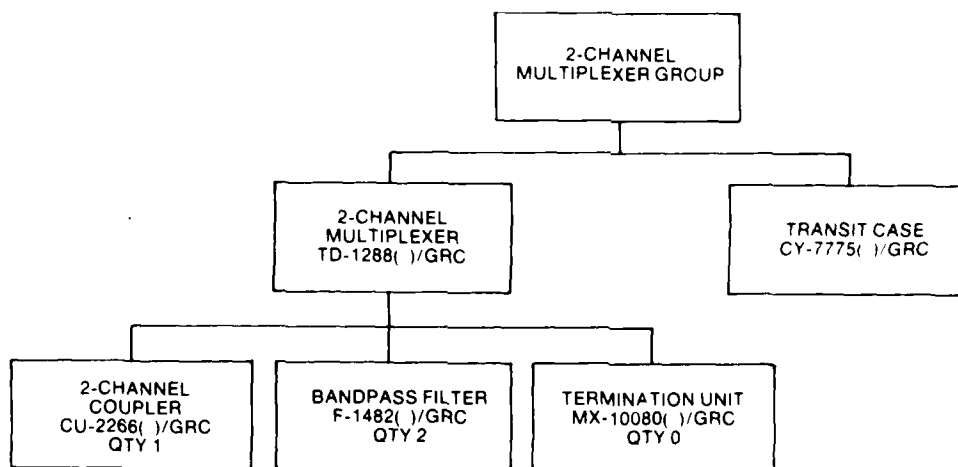


Figure 1-1.d VHF Multiplexer Family Tree.

Although the 2-channel multiplexer would perform satisfactorily with one termination unit and one bandpass filter, this is not an approved US Army configuration and it does not have an assigned nomenclature.

In this section the basic ideas and design concepts used in developing the deliverable equipments are discussed. The theoretical basis is formulated, and measured data is presented, thereby verifying achievement of performance in consonance with theory. The information and concepts have been formulated over a period of several years, and are summarized in this section.

2.1 PRELIMINARY CONSIDERATIONS

A primary design goal was to develop a multiplexer that would allow operation of up to 10 transceivers on a single broadband antenna in the 30-MHz to 88-MHz frequency range. This has been accomplished by using a selective filter in each communication channel and connecting the filter outputs in parallel through an appropriate combining/matching network. Since various multiplexer configurations (number of channels) are desired, it was advantageous to use an identical filter design in all configurations. Also the matching combining networks were developed to retain commonality in design.

Figure 2-1 depicts the basic configuration employed. The matching network is installed in a mounting base. The filters are removable, individually, from the mounting base. Push-on connectors provide the rf connection between the filters and the matching network.

2.2 FILTER DESIGN

The first area of concern was the overall filter design. The specification requires the multiplexers to provide 40 dB of port-to-port attenuation at a frequency spacing of five percent. It is also required that the filters have the lowest possible insertion loss in a minimum volume. To achieve the best possible selectivity versus insertion loss a minimum-loss design was used. The approach in determining the performance parameters and arriving at an optimum design is detailed below.

The filter is composed of parallel-tuned circuits or resonators of quantity n . The resonators are coupled together by $n-1$ coupling elements. It has been shown that the minimum-loss condition occurs when all elements of the filter are equal.¹ Thus, the equivalent circuit for all resonators comprising the filter is as shown in figure 2-2.

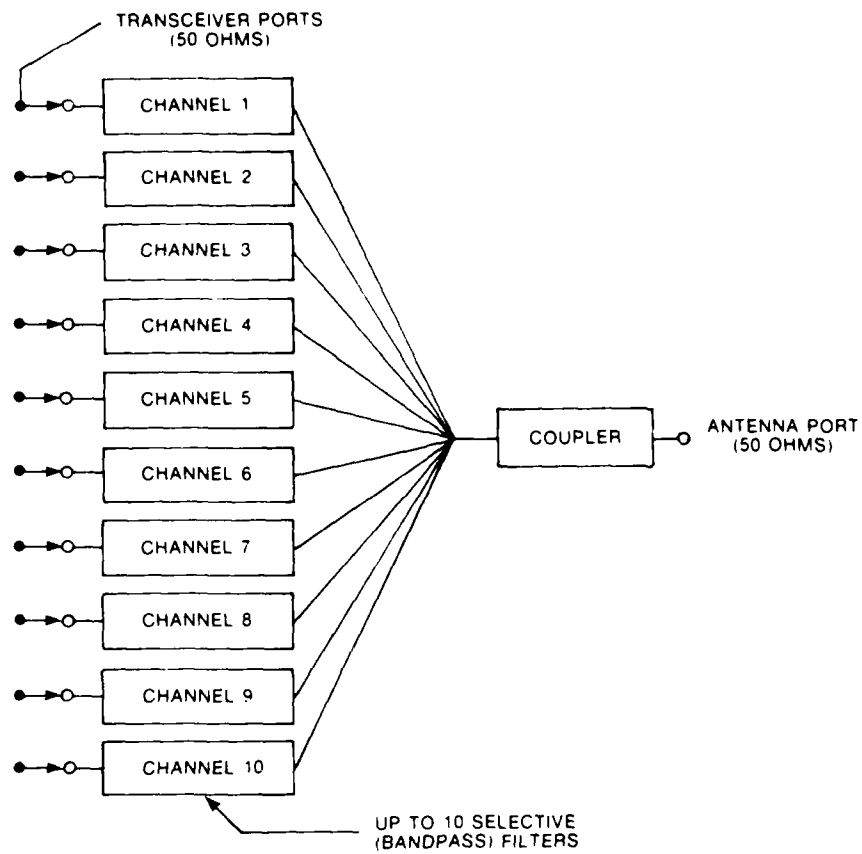


Figure 2-1. Multiplexer, Block Diagram.

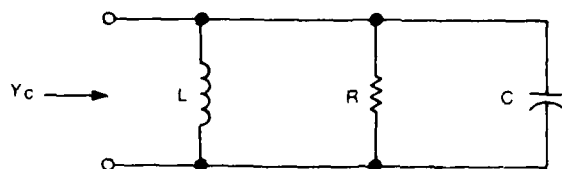


Figure 2-2. Resonator Equivalent Circuit.

The resonant frequency is:

$$\omega_o = \frac{1}{\sqrt{LC}}$$

The unloaded Q of the resonator is defined as:

$$Q_u = R\omega_o C = \frac{R}{\omega_o L}$$

The admittance of the circuit is:

$$Y_c = \frac{1}{R} + j \left(\omega C - \frac{1}{\omega L} \right)$$

The resonators are combined as shown in figure 2-3 to form a filter network.

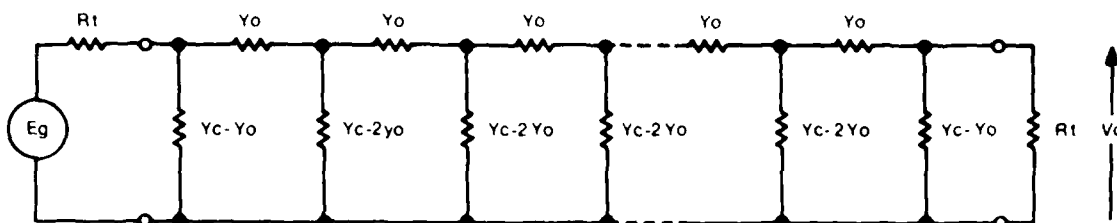


Figure 2-3. Filter With n Resonators, Equivalent Circuit.

Note

The above network has been synchronously tuned as indicated. All but the two end shunt elements are equal to $Y_c - 2Y_o$, and all series elements are equal to Y_o . There are $n-1$ series elements and $n-2$ equal shunt elements.

The resonators are coupled together by an admittance Y_o . Capacitive coupling is assumed, that is:

$$Y_o = j\omega C_o$$

The type of coupling element used in the analysis is immaterial because of the narrow bandwidth of the filter. Any form of coupling would give the same result for a filter having a bandwidth of 10 percent or less.

A terminal Q is defined, that is, the Q of the end resonators loaded by the terminating resistance only, and is given by:

$$Q_t = \frac{R_t}{\omega_o L} = R_t \omega_o C$$

The coupling coefficient is:

$$k = \frac{C_o}{C} = \frac{1}{Q_t} \sqrt{1 + \frac{Q_t}{Q_u}}$$

Because of the very narrow bandwidth of the filter, the following approximation is used:

$$U = \frac{\omega - \omega_o}{\omega} \approx -\frac{\omega}{\omega_o} - \frac{\omega_o}{\omega} \text{ where: } U \ll 1$$

Thus, the admittance of the resonator becomes:

$$Y_c = G_t \left[\frac{Q_t}{Q_u} + j2Q_t U \right]$$

The coupling admittance in the same terms is:

$$Y_o = jG_t k Q_t = jG_t \sqrt{1 + \frac{Q_t}{Q_u}}$$

The two port network shown in figure 2-3 may be redrawn as shown in figure 2-4.

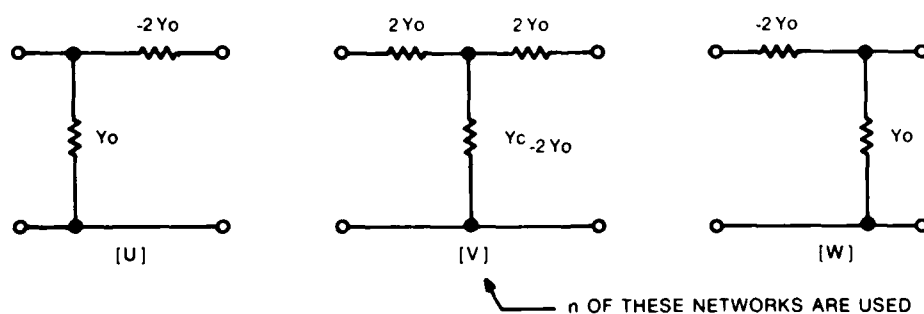


Figure 2-4. Filter With n Resonators, Resultant Equivalent Circuit.

Using ABCD matrices ², U, V, and W become:

$$U = \begin{bmatrix} 1 & 0 \\ Y_o & 1 \end{bmatrix} \begin{bmatrix} 1 & -\frac{1}{2Y_o} \\ 0 & 1 \end{bmatrix} = \begin{bmatrix} 1 & -\frac{1}{2Y_o} \\ Y_o & 1/2 \end{bmatrix}$$

$$V = \begin{bmatrix} 1 & \frac{1}{2Y_o} \\ 0 & 1 \end{bmatrix} \begin{bmatrix} 1 & 0 \\ Y_c - 2Y_o & 1 \end{bmatrix} \begin{bmatrix} 1 & \frac{1}{2Y_o} \\ 0 & 1 \end{bmatrix} = \begin{bmatrix} \frac{Y_c}{2Y_o} & \frac{1}{2Y_o} + \frac{Y_c}{4Y_o^2} \\ Y_c - 2Y_o & \frac{Y_c}{2Y_o} \end{bmatrix}$$

$$W = \begin{bmatrix} 1 & -\frac{1}{2Y_o} \\ 0 & 1 \end{bmatrix} \begin{bmatrix} 1 & 0 \\ Y_o & 1 \end{bmatrix} = \begin{bmatrix} 1/2 & -\frac{1}{2Y_o} \\ Y_o & 1 \end{bmatrix}$$

The complete network matrix is:

$$X = UV^nW$$

Examining the matrix V,

$$\text{Det } V = AD - BC = \left(\frac{Y_c}{2Y_o} \right)^2 - (Y_c - 2Y_o) \left(\frac{1}{2Y_o} + \frac{Y_c}{4Y_o^2} \right) = 1$$

Thus, by the Cayley Hamilton Theorem³, V^n may be written as:

$$V^n = S_1 V - S_2$$

$$\text{where: } S_1 = \frac{\sin n\theta}{\sin \theta}, S_2 = \frac{\sin (n-1)\theta}{\sin \theta}, \cos \theta = \frac{Y_c}{2Y_o}$$

Thus:

$$X = UV^nW = S_1 UVW - S_2 UW$$

$$X = S_1 \begin{bmatrix} 1 & -\frac{1}{2Y_o} \\ Y_o & \frac{1}{2} \end{bmatrix} \begin{bmatrix} \frac{Y_c}{2Y_o} & \frac{1}{2Y_o} & \frac{Y_c}{4Y_o^2} \\ Y_c - 2Y_o & \frac{Y_c}{2Y_o} \end{bmatrix} \begin{bmatrix} \frac{1}{2} & -\frac{1}{2Y_o} \\ Y_o & 1 \end{bmatrix}$$

$$-S_2 \begin{bmatrix} 1 & -\frac{1}{2Y_o} \\ Y_o & \frac{1}{2} \end{bmatrix} \begin{bmatrix} \frac{1}{2} & -\frac{1}{2Y_o} \\ Y_o & 1 \end{bmatrix}$$

$$X = S_1 \begin{bmatrix} 1 & \frac{1}{2Y_o} \\ Y_c - Y_o & \frac{1}{2} + \frac{Y_c}{2Y_o} \end{bmatrix} \begin{bmatrix} \frac{1}{2} & -\frac{1}{2Y_o} \\ Y_o & 1 \end{bmatrix} - S_2 \begin{bmatrix} 0 & -\frac{1}{Y_o} \\ Y_o & 0 \end{bmatrix}$$

$$X = S_1 \begin{bmatrix} 1 & 0 \\ Y_c & 1 \end{bmatrix} - S_2 \begin{bmatrix} 0 & -\frac{1}{Y_o} \\ Y_o & 0 \end{bmatrix} = \begin{bmatrix} S_1 & \frac{S_2}{Y_o} \\ S_1 Y_c - S_2 Y_o & S_1 \end{bmatrix}$$

The insertion loss of a network in terms of the ABCD parameters is:

$$L = 10 \log \frac{1}{4} \left| A + D + BG_t + \frac{C}{G_t} \right|^2$$

Therefore:

$$L = 10 \log \frac{1}{4} \left| \left(2 + \frac{Y_c}{G_t} \right) S_1 + \left(\frac{G_t}{Y_o} - \frac{Y_o}{G_t} \right) S_2 \right|^2$$

The loss in the stopband (L_s) is found from the above equation by assuming that the dissipation loss of the filter offers negligible loss as compared to the selectivity loss; that is, the unloaded Q is infinite.

Thus:

$$Y_c = j2G_t Q_t U$$

$$Y_o = jG_t$$

$$\cos \theta = Q_t U$$

The stopband loss is:

$$L_s = 10 \log \frac{1}{4} \left| (2 + j2Q_t U) \frac{\sin n\theta}{\sin \theta} - j2 \frac{\sin (n-1)\theta}{\sin \theta} \right|^2$$

$$L_s = 10 \log \left[1 - \sin^2 n\theta + \frac{\sin^2 n\theta}{\sin^2 \theta} \right]$$

$$L_s = 10 \log \left[\frac{1 - \cos^2 \theta \cos^2 n\theta}{1 - \cos^2 \theta} \right]$$

The stopband loss may be written as:

$$L_s = 10 \log \frac{1 - a^2 T_n^2(a)}{1 - a^2} \quad \text{where: } a = Q_t U$$

and: $T_n(a)$ is the Tchebycheff polynomial of the first kind.

The above equation gives the stopband attenuation for the minimum loss filter employing any number (n) of resonators. Expansion of the equation results in the following expressions for various values of n :

$$n = 1, L_s = 10 \log \frac{1}{4} [b^2 + 4]$$

$$n = 2, L_s = 10 \log \frac{1}{4} [b^4 + 4]$$

$$n = 3, L_s = 10 \log \frac{1}{4} \left[b^2 (b^2 - 1)^2 + 4 \right]$$

$$n = 4, L_s = 10 \log \frac{1}{4} \left[b^4 (b^2 - 2)^2 + 4 \right]$$

$$n = 5, L_s = 10 \log \frac{1}{4} \left[b^2 (b^4 - 3b^2 + 1)^2 + 4 \right]$$

$$n = 6, L_s = 10 \log \frac{1}{4} \left[b^4 (b^4 - 4b^2 + 3)^2 + 4 \right]$$

Where: $b = 2Q_t U$

For the specified vhf filter, the specified stopband loss, $L_s = 40$ dB, and $U = 0.05$, corresponding to a 5-percent frequency spacing the required terminal Q to achieve this selectivity is computed from the previous equations and shown in table 2-1.

Table 2-1. Terminal Q Versus Number of Resonators.

N	Q_t
1	2000.0
2	141.4
3	59.0
4	40.2
5	31.0
6	27.0

The loss in the passband (L_o) is found from the general loss expression when the circuit is resonant at the operating frequency, $U = 0$. For this case the equations become:

$$Y_c = G_t \left(\frac{Q_t}{Q_u} \right)$$

$$Y_o = jG_t \sqrt{1 + \frac{Q_t}{Q_u}}$$

$$\cos \theta = \frac{Q_t/Q_u}{j_2 \sqrt{1 + \frac{Q_t}{Q_u}}}$$

$$L_o = 10 \log \frac{1}{4} \left(2 + \frac{Q_t}{Q_u} \right)^2 \left| S_1 + \frac{S_2}{j \sqrt{1 + \frac{Q_t}{Q_u}}} \right|^2$$

The passband loss expression may be simplified to read:⁴

$$L_o = 10 \log \frac{1}{4} \left(2 + \frac{Q_t}{Q_u} \right)^2 \left(1 + \frac{Q_t}{Q_u} \right)^{n-1}$$

A very useful approximation for $L_o < 2n$ dB is:

$$L_o = 10 n \log \left(1 + \frac{Q_t}{Q_u} \right)$$

The volume occupied by a helical resonator filter is approximately:⁵

$$V = 1.6 nS^3$$

Where: S is the dimension of one side of the resonator in inches.

In the case of the deliverable hardware, the various parameters were chosen to be:

$$n = 3, S = 2.25 \text{ inches}, V = 54.675 \text{ in}^3.$$

Holding the filter volume constant, the S dimension versus n is given in table 2-2.

Table 2-2. S-Dimension Versus Number of Resonators for a Total Filter Volume of 54.675 in³.

n	S (inches)
1	3.25
2	2.58
3	2.25
4	2.05
5	1.90
6	1.79

The unloaded Q (Q_u) of each resonator is the parallel combination of the helix unloaded Q (Q_H) and the tuning capacitor Q (Q_C):

$$Q_u = \frac{Q_H Q_C}{Q_H + Q_C}$$

The tuning capacitor Q is assumed to be 5,000. The Q of the helix is given by:⁵

$$Q_H = 60 S \sqrt{f_o}$$

Where f_o is the lowest operating frequency in MHz. The lowest operating frequency results in the worst case efficiency for the filter, thus:

$$Q_u = \frac{1650 S}{5 + 0.33 S}$$

Using the values of S given in table 2-2 results in table 2-3.

Table 2-3. Resonator Unloaded Q for a 54.675-In³ Filter.

n	Q_u
1	883
2	728
3	647
4	596
5	557
6	528

Using the value of Q_u from table 2-3 and the value of Q_t from table 2-2, the insertion loss of the filter at resonance is given in table 2-4.

Table 2-4. Insertion Loss Versus the Number of Resonators for a Minimum Loss Filter of 54.675 ln^3 , Having 40 dB of Attenuation 5 Percent From the Operating Frequency.

n	L_o (dB)
1	5.139
2	1.542
3	1.137
4	1.134
5	1.176
6	1.300

The data in table 2-4 is plotted in figure 2-5. It can be seen that a 3-resonator filter provides the best performance and least complexity for the given design constraints.

The results of this section shows that a filter employing 3 resonators ($n = 3$) yields the most efficient design in terms of physical size and performance. The terminal Q (Q_t) of each resonator is designed to have a minimum value of 59. The terminal Q is also designed to be held as constant as possible over the filters operating frequency range, so as to maintain a constant percentage bandwidth.

The value of the coupling coefficient (used for internal aperture design) calculates to a constant value of:

$$k = \frac{1}{Q_t} \sqrt{1 + \frac{Q_t}{Q_u}} \approx \frac{1}{Q_t} = \frac{1}{59} = 0.01695$$

The actual value of coupling coefficient for optimized performance determined during the development of the filter is 0.0183. The design data previously presented indicates the rationale employed in developing the F-1482()/GRC filters.

2.3 OUTPUT COUPLING

The output coupling must load the output resonator to a nearly constant terminal Q (Q_t) as the filter is tuned from 30 MHz to 88 MHz. The coupling must possess sufficient physical length to allow up to 10 filters to be grouped around the common junction point. The coupling must be such that the shunting reactance of the off-channel branches have a reasonably high value with respect to the on-channel resistive component at the junction.

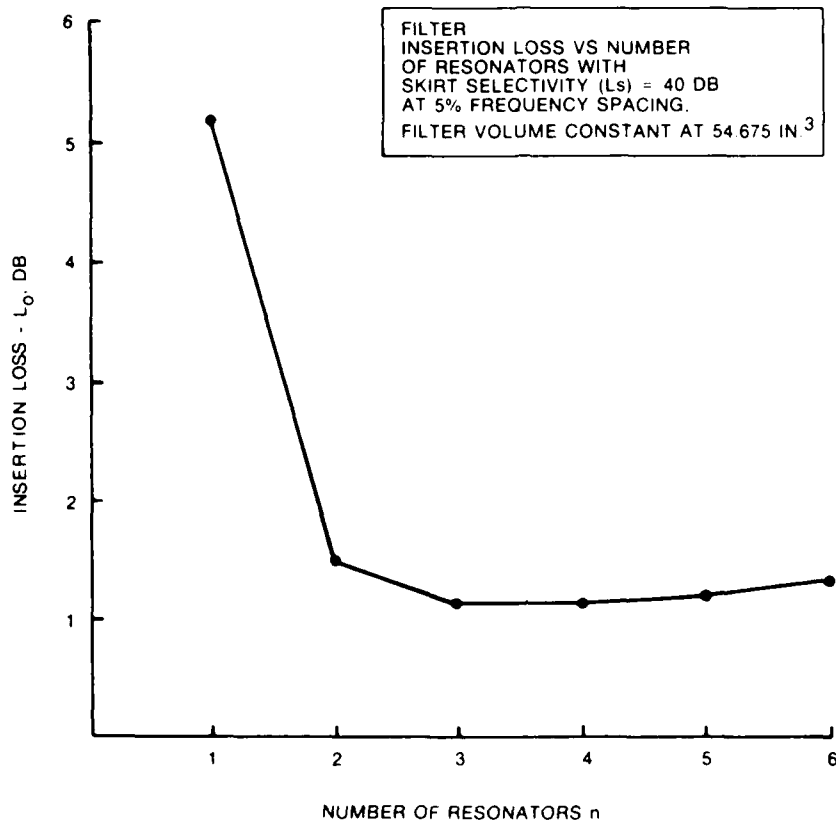


Figure 2-5. Number of Resonators Versus Insertion Loss.

Preliminary calculation indicated that the above conditions might be met by using a transmission line for the output coupling element, provided the line is used as an impedance transformer to give the proper reactance to resistance ratio at the junction. If a transmission line having a Z_0 of 50 ohms and a length of one quarter-wavelength is employed, and the on-channel resistive component is kept low ($r \approx 5$ ohms) then using the equation for a quarter-wavelength transformer:

$$Z_{in} Z_L = Z_0^2$$

the impedance level coupled into the output resonator is approximately 500 ohms. Laboratory investigation showed that the desired terminal Q (59) could not be achieved with loop coupling at the 500-ohm level. Tap coupling, however, could provide the proper loading. The total junction impedance is shown in figure 2-6.

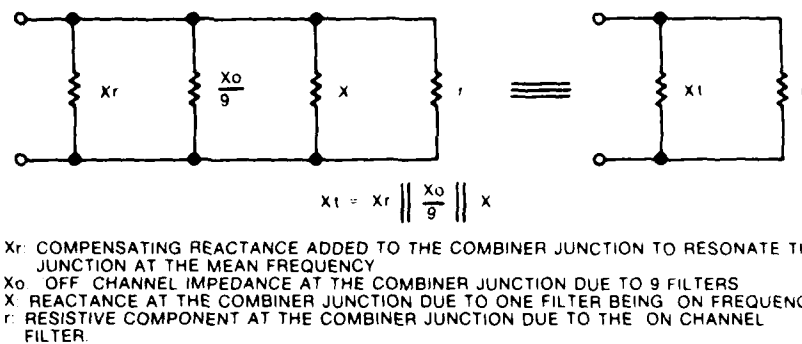


Figure 2-6. Total Junction Impedance.

The total impedance is composed of four elements in parallel. X_o represents the reactance of an off-channel branch. Since one of the channels of the multiplexer is on frequency in this analysis, the remaining nine channels form a total shunting reactance of $X_o/9$. Note that the limiting case junction problem occurs for the multiplexer configuration containing the highest number of channels, that is, ten. Thus, the analysis is performed for this case. An approximate equivalent circuit of an off-channel branch is shown in figure 2-7.

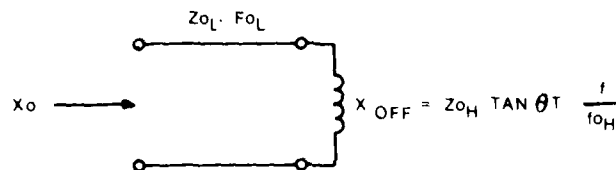


Figure 2-7. Equivalent Circuit of an Off-Channel Branch.

The circuit consists of a connecting transmission line having a characteristic impedance of Z_{OL} and a quarter-wave resonant frequency of f_{OL} . The line is terminated in the off-channel impedance of the filter (X_{OFF}). This off-channel filter impedance is assumed to be the portion of the helical output resonator from the tap point θ_t to ground, the helical resonator having a characteristic impedance of Z_{OH} and a self-resonant frequency of f_{OH} . Again, laboratory measurements confirmed that approximating X_{OFF} in this manner is a fairly valid assumption.

The on-channel branch gives two components to the total junction impedance, namely, X and r , where X is the residual reactance presented at the junction and r is the resistive component at the junction. The equivalent circuit of the on-channel branch is shown in figure 2-8.

The circuit consists of a connecting transmission line (identical to those in the off-channel branches) tapped into the output resonator at θ_t . Capacitor C tunes the output resonator to the on-channel frequency.

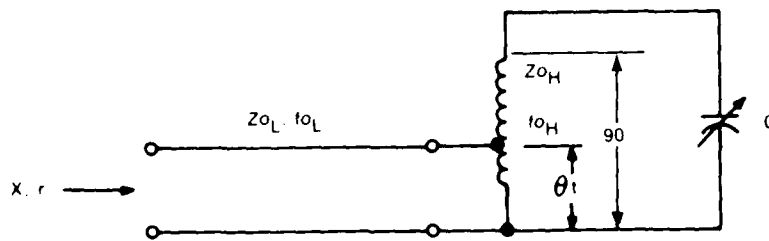


Figure 2-8. Equivalent Circuit of an On-Channel Branch.

A compensating reactance (X_T) is added to the junction so as to resonate the junction at the mean of the 30 MHz to 88 MHz band. In this case a capacitor is required to resonate the junction since the transmission lines and X_{off} are inductive. The compensating capacitor (C_T) is selected so that:

$$\left| X_T \right|_{30 \text{ MHz}} = \left| X_T \right|_{88 \text{ MHz}} = \text{reactance at the combiner junction.}$$

The junction resistance r is constant. A broadband matching network connected between the junction and the antenna terminal is used to nearly cancel the junction reactance. The effectiveness of the broadband match improves as the ratio of X_T to r increases. If the X_T/r ratio at the band edge is not appreciably less than one for the worst case (10-channel multiplexer) an efficient match may be obtained.⁷ If a suitable X_T/r ratio can be achieved for the 10-channel case, the ratio will be significantly better for multiplexers using less than 10 channels.

Given the following requirements:

- r is a constant
- $\left| X_T \right|/r$ evaluated at the band edges must be greater than 1
- Q_t as flat as possible with a minimum value of 59
- $\left| X_T \right|_{30 \text{ MHz}}$ equal to $\left| X_T \right|_{88 \text{ MHz}}$
- Z_{oL} equal 50 ohms

The following parameters must be determined:

- The characteristic impedance of the helical resonator (Z_{oH})
- The self-resonant frequency of the helical resonator (f_{oH})
- The quarter-wave resonant frequency of the connecting line (f_{oL})
- The value of r
- The angular position of the tap point (θ_t)
- The value of the compensating capacitor (C_T)

These parameters were determined by computer analysis and subsequent build and test of the resonators and filters as part of the advanced development program. During this engineering development program, new values were determined by laboratory build and test. These results then are presented in table 2-5.

Table 2-5. Optimum Parameters for Output Coupling Circuit.

ELEMENT	VALUE
Z_{off}	296 ohms
f_{off}	109.3 MHz
f_{oL}	123 MHz
r	7.2857 ohms
θt	12.5 degrees
Cr	24 pF

The analysis includes resonator and connecting line loss. The reactance of the on-channel (X) may be neglected compared to the reactance of the off channels (X_o). Using the value of f_{oL} , the physical length of the connecting transmission lines with a Teflon dielectric is 16.5 inches, which is more than adequate to permit filter interconnection.

An output resonator was constructed having a characteristic impedance of 296 ohms and a self-resonant frequency of 109.3 MHz. A connecting line was tapped into the helix. The line was a metal jacketed coax having a characteristic impedance of 50 ohms. The line length was 16.5 inches and was terminated in a 7-ohm rf load. The tap point was adjusted to give the best terminal Q characteristics. Figure 2-9 gives the results of this measurement. The resonant frequency of the connecting line (f_{oL}) was measured to be 123 MHz.

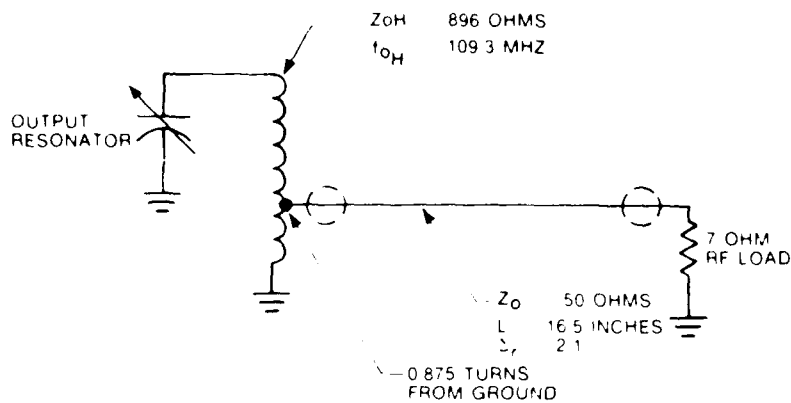
The value of the compensating capacitor (Cr) was determined experimentally to equalize the magnitude of the off-channel reactance at the band edges (30 MHz and 88 MHz) for $C_r = 24$ pF,

$$|X_t|_{30 \text{ MHz}} = |X_t|_{88 \text{ MHz}} = 48 \text{ ohms}$$

$$\text{For 10 channels, } r = 7.286\Omega \times = \frac{|X_t|}{9} = 5.333 \quad \delta_{10} = \frac{N}{r} = 0.732$$

$$\text{For 5 channels, } r = 7.286\Omega \times = \frac{|X_t|}{4} = 12.00 \quad \delta_5 = \frac{N}{r} = 1.647$$

$$\text{For 2 channels, } r = 7.286\Omega \times = \frac{|X_t|}{1} = 48.00 \quad \delta_2 = \frac{N}{r} = 6.588$$



DESIRED $Q_T = 59$ FROM 30 MHZ TO 88 MHZ

FREQUENCY MHZ	MEASURED TERMINAL Q Q_T
30	58.4
40	68.8
50	75.1
60	77.4
70	75.1
80	69.5
88	62.9

Figure 2-9. Measured Output Terminal Q.

2.4 RESONATOR DESIGN

The requirements imposed by the output coupling structure dictates that the characteristic impedance (Z_{0H}) and the self-resonant frequency (f_{0H}) of the helix both be controlled.

Existing nomographs and equation formulations do not allow simultaneous control of these two parameters. Figure 2-10 defines the various dimensions of the resonator. The design equations for the helical resonator are⁵:

$$n = \frac{1720}{f_{0H} b d} \cdot \frac{\sqrt{\log \frac{D}{d}}}{\sqrt{1 - \left(\frac{d}{D}\right)^2}} \quad \text{and: } Z_{0H} = 183 n d \left(1 - \frac{d}{D}\right) \sqrt{\log \frac{D}{d}}$$

Where:

$D = 1.2 S$ and n is in turns per inch.

Eliminating n :

$$n = \frac{1720}{f_{0H} b d} \cdot \frac{\sqrt{\log \frac{D}{d}}}{\sqrt{1 - \left(\frac{d}{D}\right)^2}} = \frac{Z_{0H}}{183 d \left(1 - \frac{d}{D}\right) \sqrt{\log \frac{D}{d}}}$$

Solving for b:

$$b = \frac{(314760) \left(1 - \frac{d}{D}\right) \log \frac{D}{d}}{f_{OH} Z_{OH} \sqrt{1 - \left(\frac{d}{D}\right)^2}}$$

The equations are most accurate when $b/d = 1.5$, therefore:

$$df_{OH} Z_{OH} \sqrt{1 - \left(\frac{d}{D}\right)^2} = (209840) \left(1 - \frac{d}{D}\right) \log \frac{D}{d}$$

where f_{OH} is in MHz

For the particular problem at hand:

$$f_{OH} = 109.3 \text{ MHz}$$

$$Z_{OH} = 296 \text{ ohms}$$

$$D = 1.2 S = (1.2) (2.25) = 2.7 \text{ inches}$$

Thus:

$$x \sqrt{1 - x^2} = k (1 - x) \log \frac{1}{x} \quad x = \frac{d}{2.7}$$

$$k = 2.40222$$

Solving for x gives:

$$x = 0.47101$$

Then:

$$d = 2.7x = (2.7) (0.47101) = 1.2717 \text{ inches}$$

$$b = 1.5d = (1.5) (1.2717) = 1.9076 \text{ inches}$$

$$n = \frac{Z_{OH}}{183d (1 - x) \sqrt{\log \frac{1}{x}}} = \frac{296}{(183) (1.2717) (1 - 0.47101) \sqrt{\log \frac{1}{0.47101}}}$$

$$= 4.205 \text{ turns/inch}$$

$$\tau = 1/n = 0.238 \text{ inch/turn}$$

The total number of turns is:

$$N = nb = (4.205) (1.9076) = 8.021 \text{ turns}$$

The wire diameter is:⁵

$$d_o = \frac{1}{2n} = \frac{1}{(2) (4.2049)} = 0.119 \text{ inch}$$

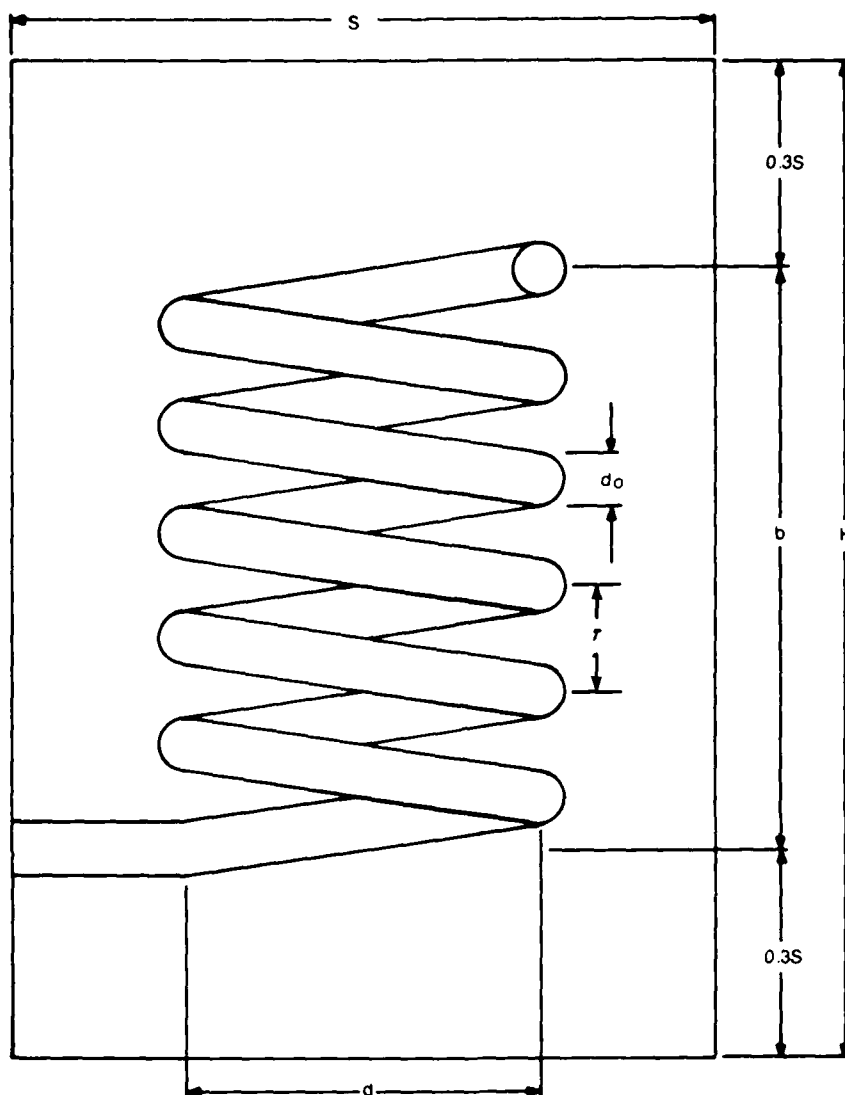


Figure 2-10. Helical Resonator Dimensions.

The helix unloaded Q is:⁵

$$Q_{Hl} = 220 D \frac{x - x^3}{1.5 - x^3} \sqrt{f_0} = (220) (1.2 S) \frac{0.47101 - (0.47101)^3}{1.5 - (0.47101)^3} \sqrt{f_0}$$

$$= 69.34 \sqrt{f_0} \text{ where } f_0 \text{ is in MHz.}$$

A helix was constructed having the following dimensions:

$$S = 2.25 \text{ inches}$$

$$d_o = 0.125 \text{ inches}$$

$$d = 1.312 \text{ inches}$$

$$\tau = 0.25$$

$$N = 6.3 \text{ turns}$$

The values for τ and d were chosen to be consistent with the advanced development models and utilize the same coil form. The number of turns in the helix was reduced from a calculated value of 8.02 turns to 6.3 turns to maintain a resonant frequency of 109.3 MHz. This was necessary due to the effects of the dielectric support, small deviations from calculated dimensions, etc.

The helix is tuned to the operating frequency range by means of a gas filled variable capacitor. The minimum required capacity is given by:

$$C_{\min} = \frac{10^6}{2 \pi f_{\max} Z_{oH} \tan \left(90^\circ \frac{f_{\max}}{f_{oH}} \right)} = \frac{10^6}{(2 \pi) (88) (296) \tan \left(90^\circ \frac{88}{109.3} \right)} = 1.931 \text{ pF}$$

The maximum required capacity:

$$C_{\max} = \frac{10^6}{2 \pi f_{\min} Z_{oH} \tan \left(90^\circ \frac{f_{\min}}{f_{oH}} \right)} = \frac{10^6}{(2 \pi) (30) (296) \tan \left(90^\circ \frac{30}{109.3} \right)} = 38.962 \text{ pF}$$

The range of the gas filled variable capacitor as employed in the deliverable hardware has a capacity range of 1.5 to 45 pF.

The maximum capacitor voltage must be calculated using the resonator reactance slope parameter (x) to obtain the equivalent inductive resistance (X_{Le}).

At 30 MHz:

$$\theta_o = 90^\circ \frac{f}{f_{oH}} = 90^\circ \frac{30}{109.3} = 24.703 = 0.4311 \text{ radians}$$

$$x = \frac{1}{2} + \frac{\theta_o}{\sin 2 \theta_o} = 0.5 + \frac{0.4311}{\sin 49.406^\circ} = 1.0677$$

$$X_{Le} = \frac{Z_{oH} \tan \theta_o}{x} = \frac{296 \tan 24.703^\circ}{1.0677} = 127.53 \text{ ohms}$$

At 88 MHz:

$$\theta_o = 90^\circ - \frac{f}{f_{OH}} = 90^\circ - \frac{88}{109.3} = 72.461 = 1.265 \text{ radians}$$

$$\lambda = \frac{1}{2} + \frac{\theta_o}{\sin 2\theta_o} = 0.5 + \frac{1.265}{\sin 144.922} = 2.701$$

$$X_{Le} = \frac{Z_{0H} \tan \theta_o}{\lambda} = \frac{296 \tan 72.461^\circ}{2.701} = 346.75 \text{ ohms}$$

The peak capacitor voltage is:

$$E_p = \sqrt{2PQ_t X_{Le}} \quad P = 60 \text{ watts}$$

$$\text{At 30 MHz: } E_p = \sqrt{(2)(60)(59)(127.53)} = 950.22 \text{ volts}$$

$$\text{At 88 MHz: } E_p = \sqrt{(2)(60)(59)(346.75)} = 1566.8 \text{ volts}$$

The gas filled variable capacitor as employed in the deliverable hardware has a minimum rf voltage rating of 3000 volts. The capacitor rms current is found from:

$$I_c = \frac{E_p}{\sqrt{2} X_c}$$

At 30 MHz:

$$I_c = \frac{950.22}{\sqrt{2} \left[\frac{10^6}{2\pi(30)(38.962)} \right]} = 4.934 \text{ amperes}$$

At 88 MHz:

$$I_c = \frac{1566.84}{\sqrt{2} \left[\frac{10^6}{2\pi(88)(1.931)} \right]} = 1.183 \text{ amperes}$$

The gas filled variable capacitor employed in the deliverable hardware is rated at 15 amperes.

The helix surface area is:

$$A = \pi db = \pi (1.312)(1.575) = 6.492 \text{ square inches}$$

The power dissipated in each resonator is approximately:

$$P_d = \frac{P}{n} \left(1 - \frac{1}{\text{antilog} \left(L_o 10 \right)} \right) = \frac{60}{3} \left(1 - \frac{1}{\text{antilog} \left(\frac{1.137}{10} \right)} \right)$$

This results in a power density on the surface of the helix of

$$\frac{4.606}{6.492} = 0.709 \text{ watt in}^2$$

This power density is below the recommended maximum of 1 watt per square inch.

The complete resonator (helix, dielectric support, and capacitor) have a measured temperature coefficient of less than -20 ppm /°C for a 75 °C temperature range. The measured unloaded Q (Qu) of the resonator is given in table 2-6.

Table 2-6. Resonator Measured Unloaded Q.

F _o , MHz	Qu
30	610
40	688
50	749
60	787
70	821
80	847
88	850

2.5 MATCHING NETWORK DESIGN

From paragraph 2.3, the design of the output coupling structure required an rf load resistance (r) of seven ohms to achieve a suitable x/r ratio at the common junction point.

The matching network design is thus divided into two distinct tasks. One, a broadband impedance transformation network to translate a 7-ohm resistive load to a 50-ohm resistive load (antenna impedance). And, two, a reactance canceling network to optimize the vwsr across the operating frequency range.

A network is used for the resistance transformation rather than a broadband iron core transformer because of the nonlinearities common to the transformer design. IMD and harmonic distortion would be severe in an iron core design since the network must handle as high as 600 watts in the 10-channel case. The word "transformer" is used in this discussion as a matter of convenience and refers to a network that provides impedance transformation.

The transformer is derived from a bandpass filter design having Tchebycheff characteristics. The passband bandwidth must be at least 58 MHz wide; for example, the transformer must operate from 30 MHz to 88 MHz. The input impedance is seven ohms when the output is terminated in 50 ohms over the passband bandwidth. Selectivity of the network is immaterial. The transformer action is incorporated into the network by repeated use of Norton's first transformation as shown in figure 2-11.

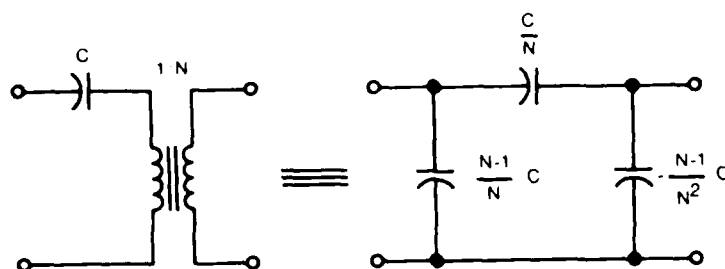


Figure 2-11. Norton's First Transformation.

Preliminary calculations indicated that a 4-pole network ($n = 4$) would be required to achieve a good match over the required frequency range.

The initial form of the network and the transformations are depicted in figure 2-12. The last circuit in figure 2-12 shows the final form of the transformer. The next step is to evaluate the elements comprising the network. Since a good match is desired across the frequency range, a low vswr Tchebycheff prototype is selected. Let the passband ripple (L_{AR}) be 0.01 dB, this corresponds to a vswr of 1.1:1. The g parameters are:²

$$g_0 = 1.0000, g_1 = 0.7128, g_2 = 1.2003, g_3 = 1.3212, g_4 = 0.6476$$

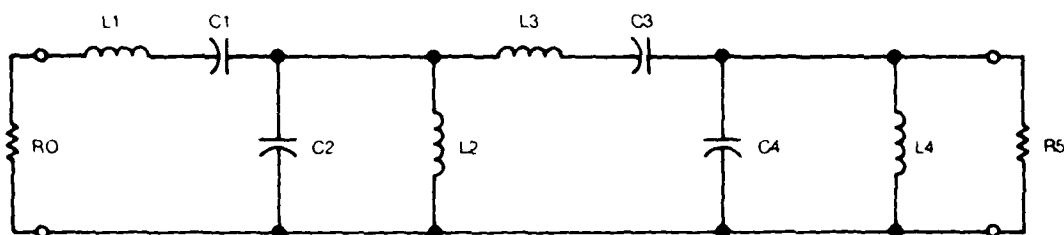
$$g_5 = 1.1007, \omega_1 = 1.0000, L_{AR} = 0.01 \text{ dB}, n = 4$$

It is also known that:

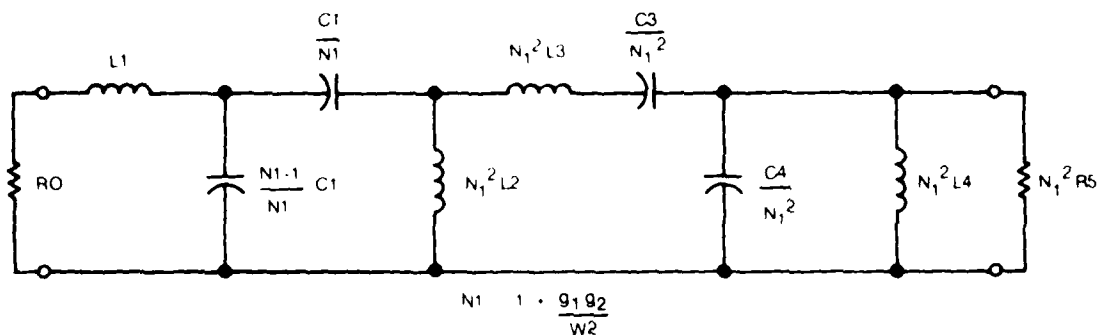
$$R_0 = \frac{51}{7} = 7.2857 \text{ ohms}, N^4 R_5 = 50 \text{ ohms}$$

Also:

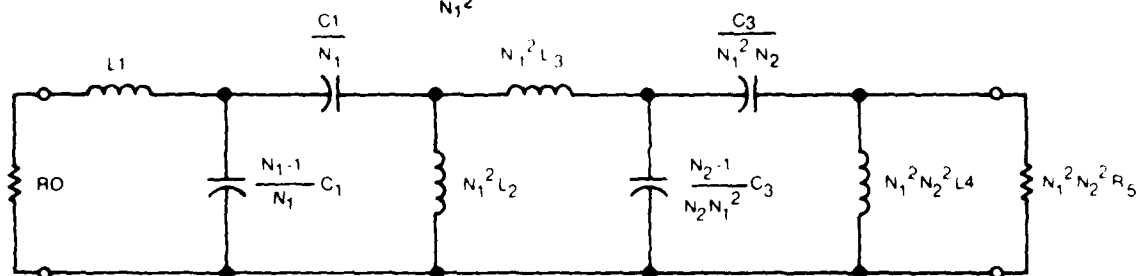
$$N^4 R_5 = N^4 R_0 g_5 = 50$$



APPLY NORTON'S TRANSFORMATION TO C_1 SUCH THAT C_2 IS ABSORBED



APPLY NORTON'S TRANSFORMATION TO $\frac{C_3}{N_1^2}$ SUCH THAT C_4/N_1^2 IS ABSORBED



FOR A TCHEBYCHEFF DESIGN IT IS KNOWN THAT $g_1 g_2 = g_3 g_4$ THEREFORE $N_1 = N_2 = N$
THUS

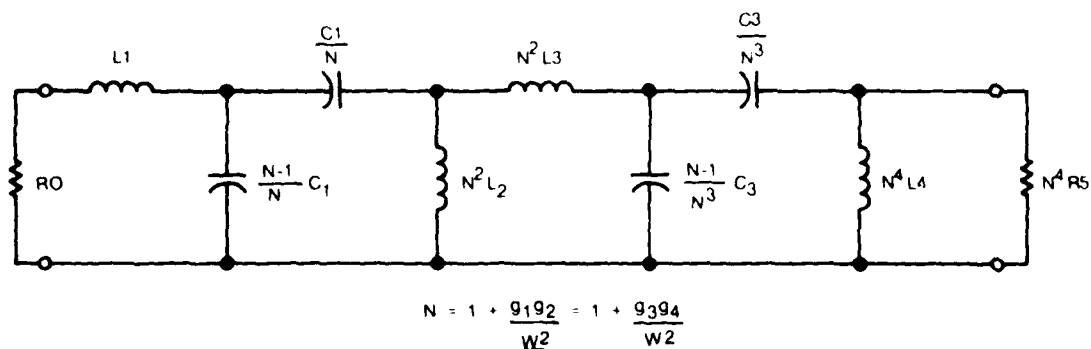


Figure 2-12. Reduction of Transformer to Final Form.

The equivalent transformer turns ratio (N) is therefore:

$$N = \left(\frac{50}{R_{085}} \right)^{\frac{1}{4}} = \left[\frac{50}{(7.2857)(1.1007)} \right]^{\frac{1}{4}} = 1.5802$$

From figure 2-12 the fractional bandwidth (w) may be found as:

$$w = \sqrt{\frac{R_1 R_2}{N-1}} = \sqrt{\frac{(0.7128)(1.2003)}{0.5802}} = 1.2143$$

Also:

$$w = \frac{f_2 - f_1}{f_0} = \frac{f_2 - f_1}{\sqrt{f_1 f_2}}$$

For equal guardbands above 88 MHz and below 30 MHz it requires that:

$$f_2 - 88 = 30 - f_1$$

Thus:

$$f_1 = 59 \left(1 - \sqrt{\frac{w}{4 + w^2}} \right) = 28.379 \text{ MHz}$$

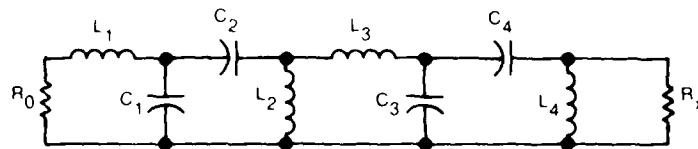
$$f_2 = 118 - f_1 = 89.621 \text{ MHz}$$

$$f_0 = \sqrt{f_1 f_2} = 50.4317 \text{ MHz}$$

$$\omega_0 = 2 \pi f_0 = 0.3169 \times 10^9 \text{ radians/second.}$$

The element values for the network shown in figure 2-12 are calculated as shown in figure 2-13. Figure 2-14 shows the final experimentally determined values.

The second design task is to determine the reactance cancellation networks. To provide reasonable element values, the cancellation networks are inserted between the broadband transformer and the antenna terminal rather than at the common junction. The design is performed for three cases; for example, a 2-channel, 5-channel, and a 10-channel multiplexer. Multiplexers containing different number of channels would have cancellation network complexity falling between those presented.



$$R_0 = 7.2857 \dots$$

$$L_1 = \frac{g_1 R_0}{\omega - \omega_0} = \frac{(0.7128)(7.2857)}{(1.2144)(0.3169)} = 13.4962 \text{ nH}$$

$$C_1 = \frac{(N-1) \omega}{g_1 \omega_0 R_0 N} = \frac{(0.5802)(1.2144)(1000)}{(0.7128)(0.3169)(7.2857)(1.5802)} = 270.9453 \text{ pF}$$

$$C_2 = \frac{\omega}{g_1 R_0 \omega_0 N} = \frac{(1.2144)(1000)}{(0.7128)(7.2857)(0.3169)(1.5802)} = 467.005 \text{ pF}$$

$$L_2 = \frac{N^2 \omega R_0}{g_2 \omega_0} = \frac{(2.4970)(1.2144)(7.2857)}{(1.2003)(0.3169)} = 58.0846 \text{ nH}$$

$$L_3 = \frac{g_3 R_0 N^2}{\omega - \omega_0} = \frac{(1.3212)(7.2857)(2.4970)}{(1.2144)(0.3169)} = 62.4634 \text{ nH}$$

$$C_3 = \frac{(N-1) \omega}{g_3 \omega_0 R_0 N^3} = \frac{(0.5802)(1.2144)(1000)}{(1.3212)(0.3169)(7.2857)(3.9457)} = 58.5419 \text{ pF}$$

$$C_4 = \frac{\omega}{g_3 R_0 \omega_0 N^3} = \frac{(1.2144)(1000)}{(1.3212)(0.3169)(7.2857)(3.9457)} = 100.9026 \text{ pF}$$

$$L_4 = \frac{\omega R_0 N^4}{g_4 \omega_0} = \frac{(1.2144)(7.2857)(6.2349)}{(0.6476)(0.3169)} = 268.8178 \text{ nH}$$

$$R_x = g_5 N^4 R_0 = (1.1007)(6.2349)(7.2857) = 50 \text{ OHMS}$$

THE FINAL COMPUTED NETWORK USING STANDARD VALUE CAPACITORS BECOMES

Figure 2-13. Broadband Transformer Calculations (Part 1).

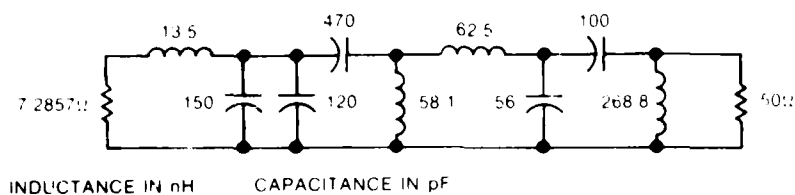
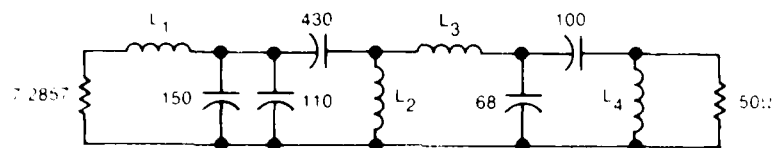
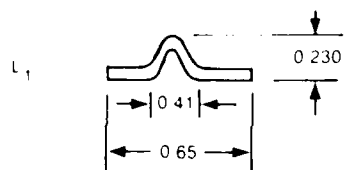


Figure 2-13. Broadband Transformer Calculations (Part 2).



ALL INDUCTORS FORMED WITH #14 SILVER PLATED BUS



L_2 2 TURNS 0.390 ID 0.100 C-C TURNS SPACING

L_3 2 TURNS 0.390 ID 0.170 C-C TURNS SPACING

L_4 5 TURNS 0.510 ID 0.104 C-C TURNS SPACING

Figure 2-14. Broadband Transformer, Final Values.

From Fano's work,⁶ a minimum insertion loss network results when:

$$\frac{\tanh na}{\cosh a} = \frac{\tanh nb}{\cosh b}$$

where: $d = \sinh a$

$e = \sinh b$

$$e = d - 2 \delta \sin \frac{\pi}{2n}$$

In the above equations n is the number of elements comprising the low-pass prototype network. $n = 1$ is the case where no matching network is required. δ is the x/r ratio evaluated at the band edges.

The maximum passband loss $(L_A)_{\max}$ is evaluated in the following manner:

For, $n = 1$: $d = \sinh a$, $e = \sinh b$, $e = d - 2\delta$

$$\frac{\tanh a}{\cosh a} = \frac{\tanh b}{\cosh b} \rightarrow \frac{\sinh a}{\cosh^2 a} = \frac{\sinh b}{\cosh^2 b} \rightarrow \frac{\sinh a}{1 + \sinh^2 a} = \frac{\sinh b}{1 + \sinh^2 b}$$

$$\rightarrow \frac{d}{1 + d^2} = \frac{e}{1 + e^2} \rightarrow \frac{d}{1 + d^2} = \frac{d - 2\delta}{1 + d^2 - 4\delta d + 4\delta^2}$$

For the 2-channel multiplexer:

$\delta = \delta_2 = 6.588$ (from section 2.3), let, $n = 1$

$$(L_A)_{\max} = 10 \log \frac{\delta^2 + \delta \sqrt{\delta^2 + 1} + 1}{2\delta \sqrt{\delta^2 + 1}} = 10 \log \frac{88.307}{87.804} = 0.0248 \text{ dB}$$

$$H = 10^{\frac{(L_A)_{\max}}{10}} = 1.005727$$

$$V_{\text{swr}_{\max}} = 2H - 1 + 2 \sqrt{H(H - 1)} = 1.163:1$$

This is an excellent match. Thus we can conclude for the 2-channel case no matching network is required, and the transformer output can be connected directly to the antenna terminal.

For the 5-channel multiplexer:

$\delta = \delta_5 = 1.64706$ (from section 2.3), let, $n = 1$

$$(L_A)_{\max} = 10 \log \frac{\delta^2 + \delta \sqrt{\delta^2 + 1} + 1}{2\delta \sqrt{\delta^2 + 1}} = 10 \log \frac{6.8865}{6.3473} = 0.3541 \text{ dB}$$

$$H = 10^{\frac{(L_A)_{\max}}{10}} = 1.0849$$

$$V_{\text{swr}_{\max}} = 2H - 1 + 2 \sqrt{H(H - 1)} = 1.7770:1$$

The vswr is quite high. Try $n = 2$

$$(L/A)_{\max} = 10 \log \frac{(\delta^2 + \delta \sqrt{\delta^2 + 1} + 1)^2}{4\delta(\delta^2 + 1)^{3/2}} = 10 \log \frac{47.4236}{47.1330} = 0.0267 \text{ dB}$$

$$H = 10^{\frac{(L/A)_{\max}}{10}} = 1.006168$$

$$V_{\text{swr}}_{\max} = 2H - 1 + 2\sqrt{H(H - 1)} = 1.170:1$$

Thus it can be concluded that a single series tuned circuit (L_2 and C_2) connected between the common junction point and the transformer will provide the desired degree of matching. The element values for the 5-channel matching network are computed in figure 2-15.

5-CHANNEL MULTIPLEXER

CALCULATION OF ELEMENT VALUES FOR ADDITIONAL MATCHING SECTION

$n = 2$, $\delta = 1.64706$, $H = 1.006168$, $f_1 = 30 \text{ MHz}$, $f_2 = 88 \text{ MHz}$, $R = 50 \text{ OHMS}$

$$d = \left[\frac{\sqrt{\frac{1}{H-1}} + \sqrt{\frac{H}{H-1}}}{n} \right] \sinh \left[\frac{(12.73291 + 12.77212)}{2} \right]$$

$$\sinh 1.619438 = 2.42612$$

$$D = \frac{d}{\delta \sin \frac{\pi}{2n}} = 1 + \frac{2.42612}{1.64706 \sin \frac{\pi}{4}} = 1.08314$$

$$\text{LETTING } g_0 = 1, \frac{1}{b_1} = 1$$

$$g_1 = \frac{1}{\delta} = \frac{1}{1.64706} = 0.607142$$

$$f_0 = \sqrt{f_1 f_2} = \sqrt{(30)(88)} = 51.38093 \text{ MHz}, \omega_0 = 0.322836 \times 10^9 \text{ RAD/SEC}$$

$$u = \frac{f_2 f_1}{f_0} = \frac{58}{51.38093} = 1.128823$$

$$k_{12} = \sqrt{\frac{1 + (1 + D^2)^2}{2}} = \sqrt{\frac{1 + (2.17319)(2.71281)}{2}} = 1.85680$$

$$g_2 = \frac{1}{g_1 (k_{12})^2} = 0.47772, g_3 = \frac{1}{D \delta g_2} = 1.17335$$

$$X_L = X_C = \frac{1}{\omega_0 g_2 R} = \frac{(0.47772)(50)}{1.128823} = 21.16008 \text{ OHMS}$$

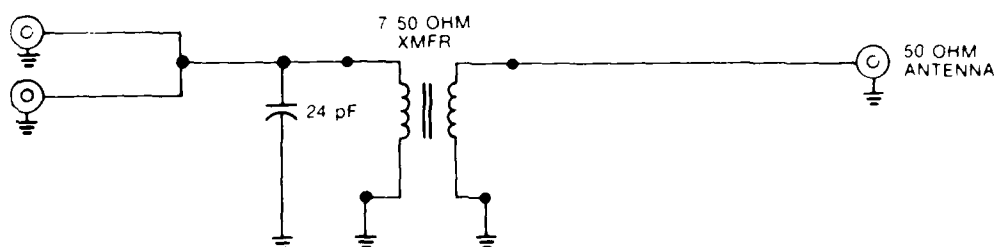
$$L = \frac{X_L}{\omega_0} = \frac{21.16008}{0.322836} = 65.544 \text{ nH}$$

$$C = \frac{1}{X_C \omega_0} = \frac{1000}{(21.16008)(0.322836)} = 146.386 \text{ pF}$$

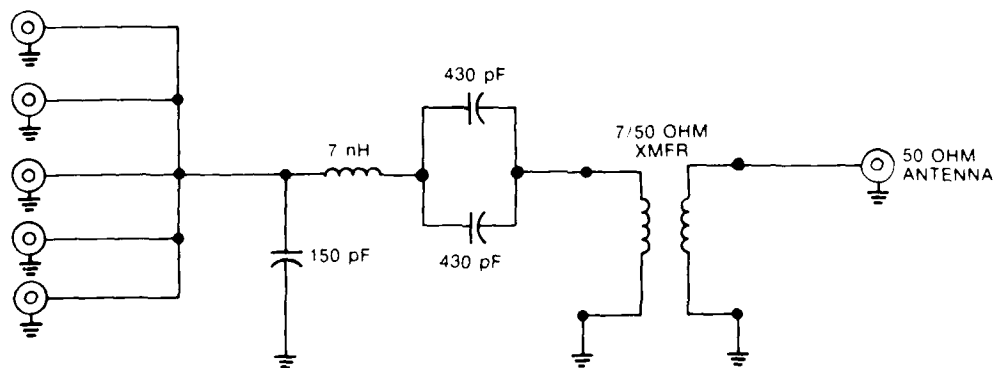
Figure 2-15. Matching Section Element Determination.

The final form of the combining/matching networks are shown in figure 2-16. Note the addition of the compensating capacitor at the common junction. This capacitor has a value of $(N - 1)C_F$ where n is the number of channels comprising the multiplexer, and C_F is equal to 24 pF (from table 2-5).

The actual component values used in the transformer and matching networks differ very slightly in the deliverable hardware (paragraph 3.4). This is due to two factors: one, standard value capacitors are used, and two, some compensation of inevitable stray capacity and inductance is required. The transformers were adjusted for a minimum return loss of 21 dB, this corresponds to a maximum vswr of 1.20:1.



2-CHANNEL MULTIPLEXER



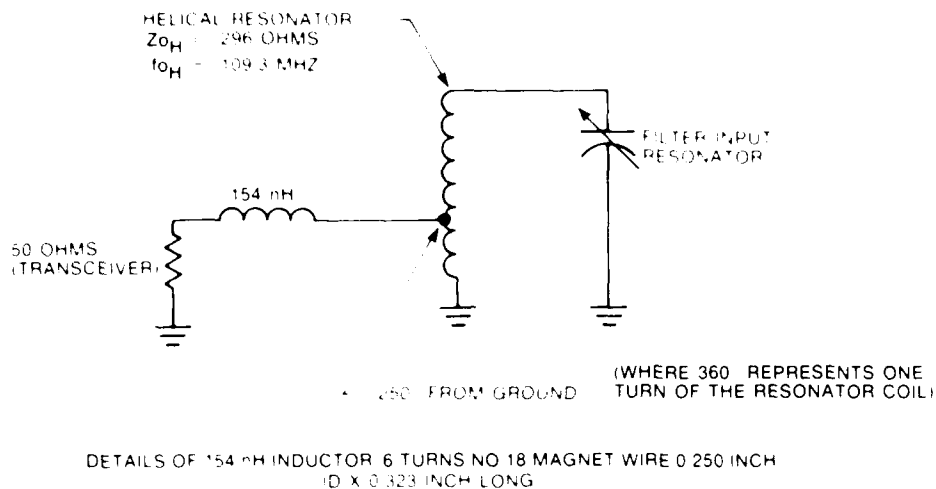
5-CHANNEL MULTIPLEXER

Figure 2-16. Final Coupler Configuration.

2.6 INPUT AND INTERNAL COUPLINGS

The input coupling arrangement has been determined experimentally. The most suitable method of several tried is a tapped coupling to the input resonator with a series compensating inductor. This arrangement gives a fairly constant terminal, $Q (Q_t)$, and causes little frequency shift to be introduced into the input resonator. The helix is tapped 250 degrees from

the ground end. The compensating inductor is composed of 6 turns of number 18 magnet wire, close wound, with a 0.25 inch ID and 0.323 inch length. The measured reactance of the compensating coil is 29 ohms at 30 MHz. Figure 2-17 presents the measured terminal Q for this configuration.

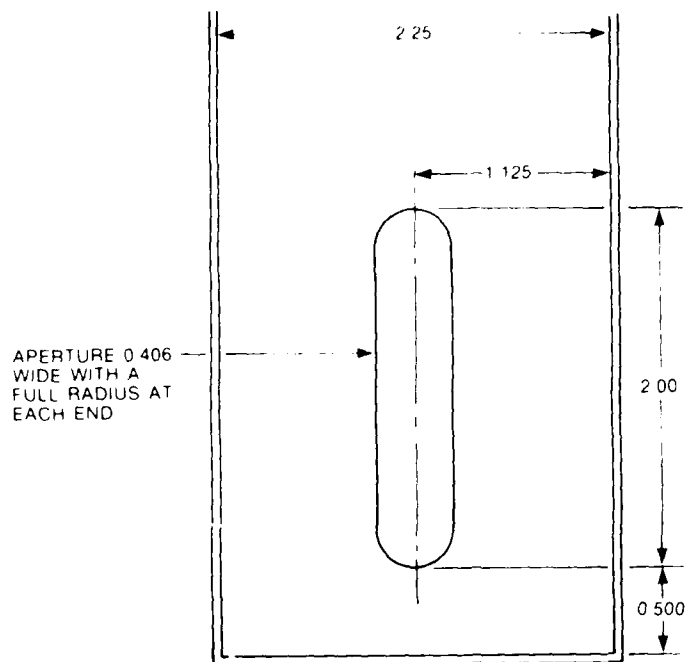


DESIRED Q_T 59 FROM 30 MHZ TO 88 MHZ

FREQUENCY MHZ	MEASURED TERMINAL Q Q_T
30	62.8
40	58.3
50	57.0
60	56.7
70	57.5
80	58.0
88	58.3

Figure 2-17. Measured Input Terminal Q.

Aperture coupling is used for the two internal couplings. This form of coupling can be made to agree very closely with the desired value. For a constant percentage bandwidth filter the coefficient of coupling should remain a constant value over the operating frequency range. In this case the magnitude of the coupling coefficient is approximately 0.017. Figure 2-18 presents the measured coupling for the depicted configuration.



DESIRED $K = 0.0183$ FROM 30 MHZ TO 88 MHZ

FREQUENCY MHZ	MEASURED K_1
30	0.0172
40	0.0175
50	0.0179
60	0.0185
70	0.0192
80	0.0199
88	0.0205

Figure 2-18. Measured Coupling Coefficient.

2.7 TUNING METHOD AND DISCRIMINATOR DESIGN

A block diagram of the filter is shown in figure 2-19. Two discriminators, a forward/reflected power discriminator (directional coupler), and a 90-degree phasing discriminator are employed to tune the filter. The use of two discriminators results in perfect tunes, that is, a symmetrical response shape.

The filter is basically tuned for minimum reflected power. The phasing function assures that the correct minimum reflected power point is used. The forward power indication is used as a monitoring function only.

Figure 2-20 shows a simplified schematic of the directional coupler. The reflected power detector operates in the following manner: a current sample is taken from the transmission line by means of a transformer. This provides a voltage across the load resistor proportional to the line current. This voltage is applied to the anode of the diode. Simultaneously a voltage sample is applied to the cathode end of the diode (derived from the capacitor

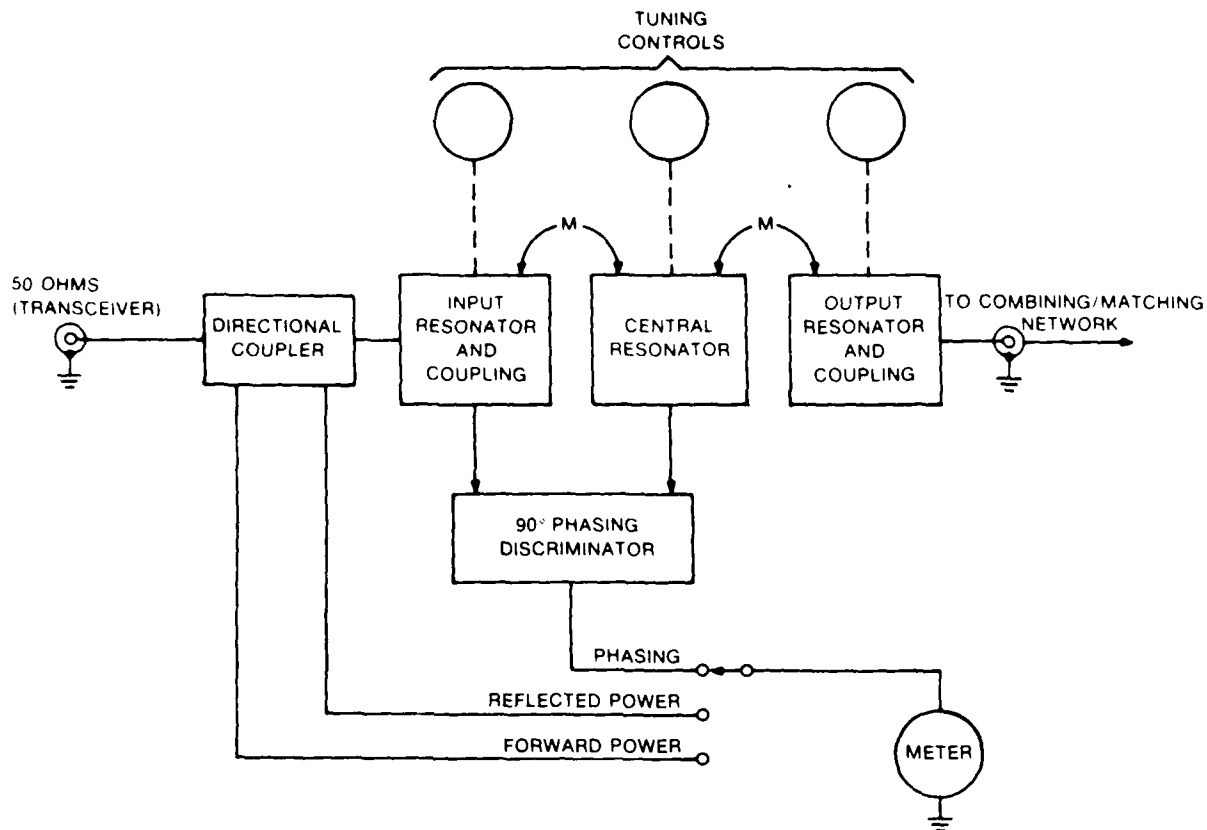


Figure 2-19. Filter, Simplified Block Diagram.

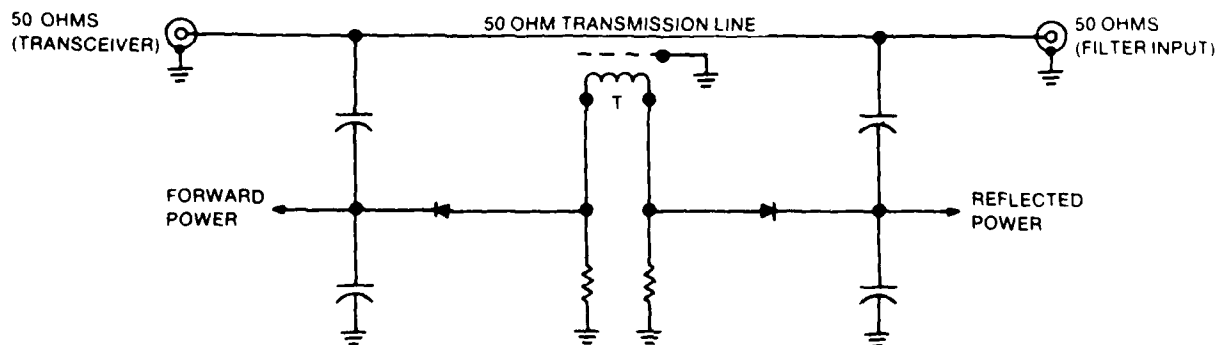


Figure 2-20. Directional Coupler, Simplified Schematic.

divider). The transformer phasing and circuit constants are set up so that when the transmission line is terminated in its characteristic impedance (50 ohms), the two samples are equal in phase and magnitude; thus, the diode does not conduct and the reflected power output is zero. Any deviation of the terminating impedance from 50 ohms causes this balance to be upset. The diode then conducts proportional to the unbalance, giving a dc output voltage proportional to reflected power. The forward power detector works in essentially the same manner except the current and voltage samples are 180 degrees out of phase. This results in the dc output voltage being a maximum when the transmission line is terminated in 50 ohms. Other values of terminating impedance cause the dc output voltage to vary proportional to the forward power.

Figure 2-21 shows a simplified schematic of the phasing discriminator. This is a conventional 90-degree discriminator. The voltage sample V_2 appears in the secondary of the transformer as two equal voltages but, 180 degrees different in phase with respect to the center tap. The second voltage sample V_1 is connected to the center tap. Thus, when V_1 and V_2 have a 90-degree relationship, the dc voltage appearing across the potentiometer is equal in magnitude and opposite in polarity with respect to the wiper of the potentiometer. The total voltage across the potentiometer is zero. As the phase relationship of the two voltages change the total voltage across the potentiometer is either positive or negative depending on whether V_1 leads or lags V_2 by more or less than 90 degrees. The magnitude depends on how greatly the angle between the two voltages differ. A bridge rectifier is connected to the output of the discriminator, this provides a unidirectional voltage output for the metering circuitry; for example, the output voltage of the bridge circuit is zero for a 90-degree phase relationship between V_1 and V_2 and positive going for any deviation from 90 degrees between the two voltage samples.

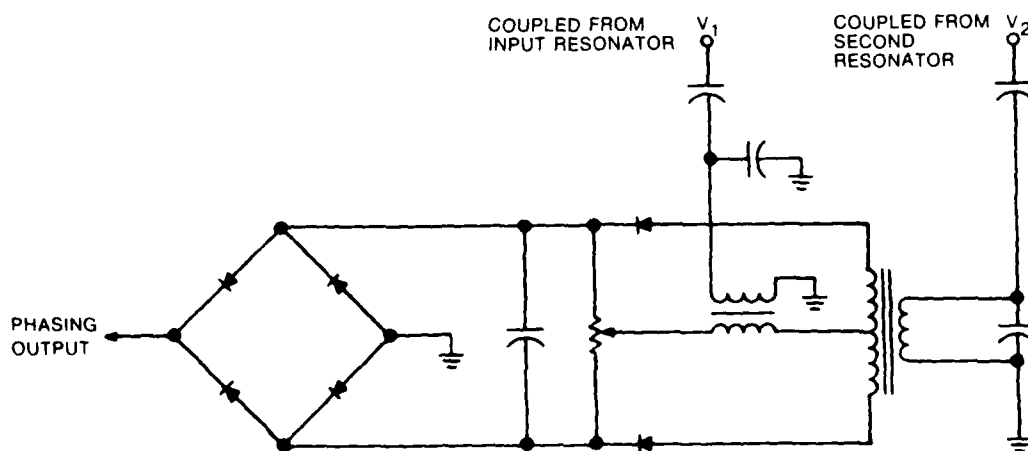


Figure 2-21. 90° Discriminator, Simplified Schematic.

Details of the 2- and 5-channel multiplexers in regard to physical configuration, electrical design, and measured performance are presented.

3.1 GENERAL DESCRIPTION

Figures 3-1 through 3-3 depicts the possible configurations of the TD-1289()/GRC Multiplexer by addition of the Termination unit MX-10080()/GRC. Figure 3-4 depicts the TD-1288()/GRC 2-channel version. They consist of identical bandpass filter modules and an appropriate coupler (mounting base) which houses the combining/matching network. An antenna connector (type N) is located on the right side of the coupler. The rf connectors (type BNC) for connection to the transceivers are located at the top of the rear surface of each bandpass filter.

Push-on rf connectors are used to connect the outputs of the bandpass filters to the matching networks located in the coupler. Figure 3-5 shows a 2-channel coupler with the filters removed.

Figure 3-6 shows a 5-channel coupler with the filters removed.

Four screws are used to retain each of the bandpass filters in its position on the coupler unit. Two screws are located on the lower front edge of the filter, the other two screws being located on the rear surface of the filter just below the transceiver connector. The controls and connectors associated with each filter are protected by panel extensions, and in the case of the output connector, by the carrying handle. The overall weight of the 2-channel multiplexer is 17 pounds maximum, while the 5-channel multiplexer overall weight is 37 pounds maximum.

Termination Unit (MX-10080()/GRC) was also developed as part of this contract. This unit can be considered a filter simulator which should be substituted for a bandpass filter when one filter position of the coupler does not contain a filter. This unit has a push-on rf connector identical to that on the bandpass filter. Two screws are used to secure it when in position (figures 3-7 and 3-8).

Each bandpass filter has three tuning knobs and associated tune frequency indicator dials. Each knob has an integral knob lock. Tuning is accomplished by setting the three knobs to the desired frequency (indicated by the frequency dials), applying rf power and fine tuning by using the power and phase selector and meter to ensure minimum reflected power and phasing error. The meter located on the top of the front panel of each filter is used to indicate forward power, reflected power, and phase error. A six-position switch to the left of the meter allows selection of these functions in either 60-watt or 6-watt ranges. (See figures 3-9 and 3-10.)

Each multiplexer is supplied with a transit case. The case is constructed of fiberglass and contains shock absorbing foam, properly shaped to protect the multiplexer when in transit. The 2-channel case contains a 4 lb/ft³ density polyurethane foam, and the 5-channel case has a stiffer 2 lb/ft³ polyethylene foam. The case has been designed and tested to protect the multiplexer from a drop of four feet. (See figures 3-11 and 3-12.)

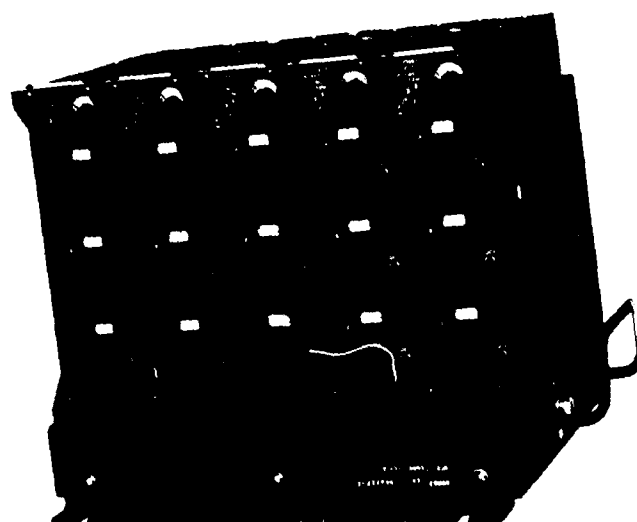


Figure 3-1. 5-Channel Multiplexer (TD-1289()(V)1/GRC).

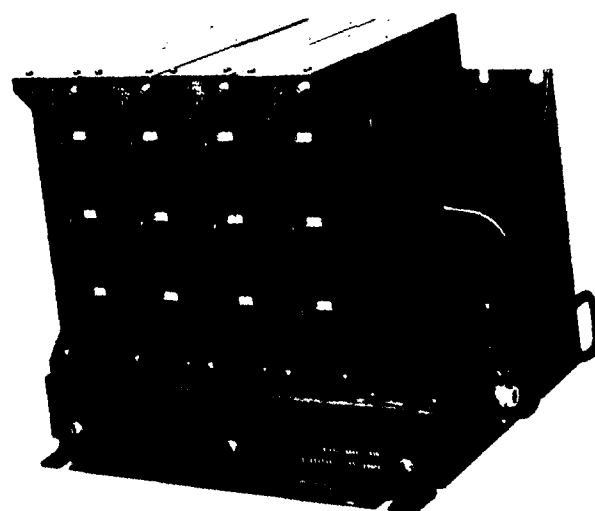


Figure 3-2. 4-Channel Multiplexer (TD-1289()(V)2/GRC).

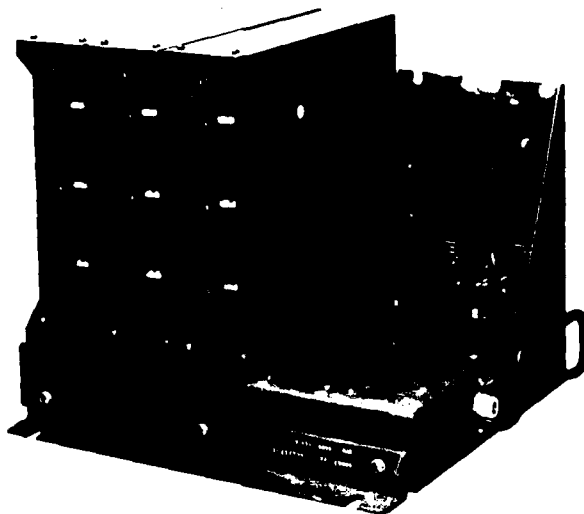


Figure 3-3. 3-Channel Multiplexer (TD-1289() (V)3 (GRC).

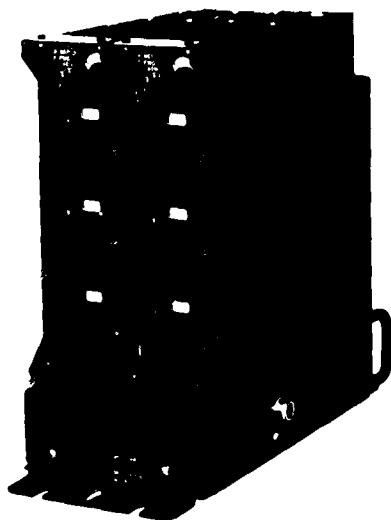


Figure 3-4. 2-Channel Multiplexer (TD-1288() (GRC).

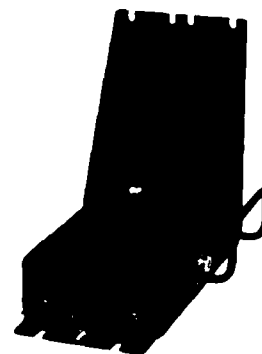


Figure 3-5. 2-Channel Coupler (CU-2266() (GRC).

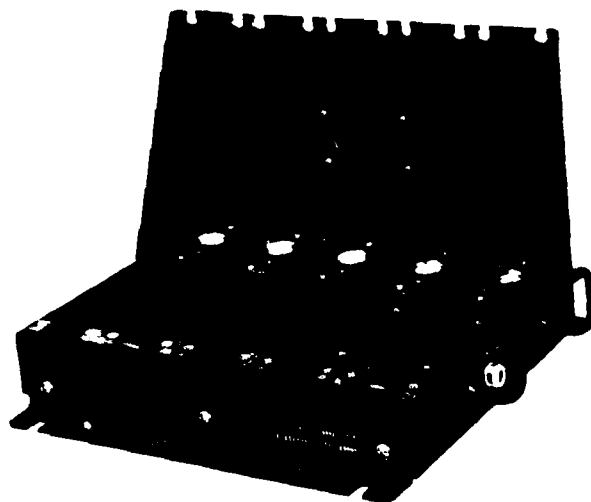


Figure 3-6. 5-Channel Coupler (CU-2267() GRC).



Figure 3-7. Termination Unit (MX-10080() GRC).

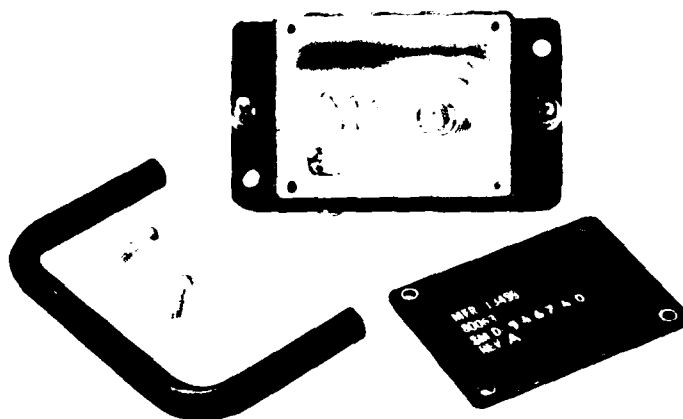


Figure 3-8. Termination Unit With Cover Removed (MX-10080() GRC).

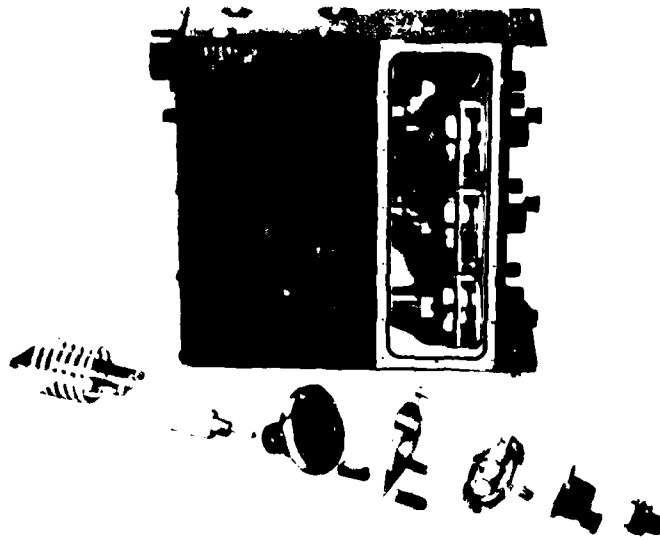


Figure 3-9. Bandpass Filter, Exploded View (F-1182() GRC).



Figure 3-10. Bandpass Filter, Rear View (F-1182() GRC).

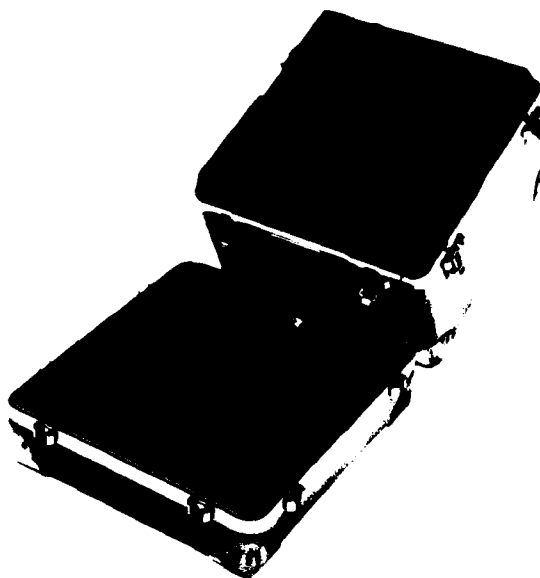


Figure 3-11. Transit Case-5-Channel Multiplexer (CY-7776() GRC).

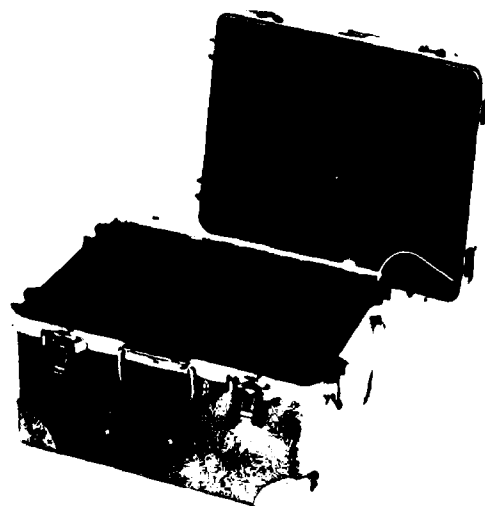


Figure 3-12. Transit Case-2-Channel Multiplexer (CY-7775() GRC).

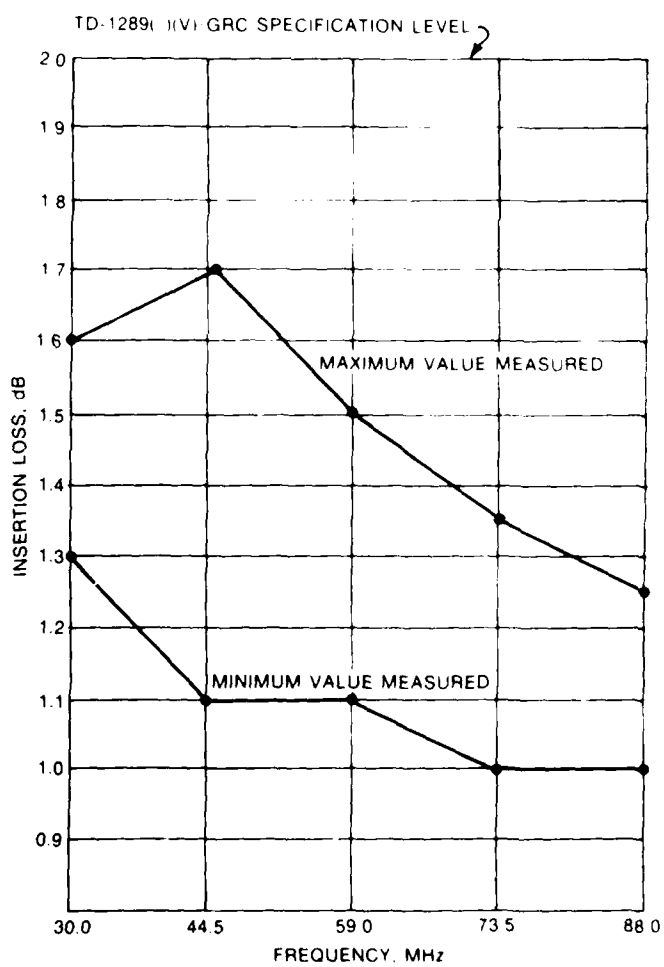


Figure 3-13. Measured Insertion Loss for the TD-1289() (V)1/GRC 5-Channel Multiplexer.

3.2 MEASURED PERFORMANCE

The measured performance parameters, including insertion loss, vswr, and transceiver port attenuation, are included and have been derived from the Engineering Accomplishment Evaluation Report. This data represents the best case and worst case data from the 10 communications channels of two multiplexers. The data found in figures 3-13 through 3-15 evolved from reference tests which were performed after the required environmental tests.

Figure 3-13 shows the minimum maximum insertion loss when measured from transceiver port to antenna port. The insertion loss measurement results lie between 1.0 and 1.7 dB.

The measured transceiver port to transceiver port attenuation is shown in figure 3-14. The data was obtained by tuning two filters to maintain a five-percent frequency spacing, injecting an on-channel signal into one filter, and measuring the feedthrough signal at the other filter. The minimum attenuation measured was 45.3 dB.

Figure 3-15 shows the voltage standing wave ratio measured at the transceiver inputs. Measurements indicated vswr variations from 1.06 to 1.58.

In addition to previous tests run under laboratory ambient conditions, a series of environmental tests were performed on one 2-channel and two 5-channel multiplexers. The tests performed included: 3:1 vswr load test, immersion, bench handling, loose cargo bounce test, transit drop, vibration (sine) (intended to verify that the equipment would withstand field transport by military vehicles), fungus, low temperature, high temperature, altitude, dust, humidity, rain, and salt fog. The results of these tests (procedures, measured data, discussion of results, etc) were presented in the Engineering Accomplishment Evaluation Report, G003 dated 21 November 1979. After incorporation of modifications to stiffen the foam in the 5-channel transit case, the unit passed the transit drop test. Both multiplexers met all the environmental test criteria specified except for the fungus requirement.

Investigation has revealed that there is no fungus inhibitor in the forest green enamel paint per MIL-E-52798A. This resulted in a random fungal growth over much of the surface of the test unit, including knobs and lock screws where organics such as oil and skin particles are easily embedded.

Unfortunately, this initial fungal growth was cause for concern and judged a failure. However, the fungal growth noted did not affect the performance of the multiplexer, and the growth was not considered excessive. No corrective action was requested by the customer, nor was any initiated by the contractor.

One problem encountered, however, during the Engineering design test was the observation of intermodulation distortion (IMD) at levels beyond those specified in US Army Electronics Command Specification EL-CP0192-0001A. The first measurements during the test indicated levels as high as 98 dB below the output carrier level due to a 60 watt input signal. (The maximum allowable specification level being 120 dB below the output carrier level.) After extensive testing and substitution of various parts of the multiplexer, it was determined that the IMD was generated by the variable capacitors located in the helical resonator cavities. By replacing the spring contact fingers inside these capacitors with those of an improved physical configuration and including a gold flash on the contact surfaces, the IMD performance specification of -120 dB was met, as evidenced by the data included in figure 3-16. However, relaxation as requested in production contract DAAK80-80-C-0262 is anticipated to ensure a manufacturable product. After verification of improved IMD performance in

these tests, the vendor specification on the variable capacitor was revised to require the gold flash on the contact surfaces. It should be noted, however, that test results indicated the required IMD performance is at levels where dirty rf connectors, nonlinear rf loads, poor assembly techniques, etc, will result in intermodulation components beyond the specified levels. In fact, this parameter will be checked and tested randomly during the first production run to verify what IMD performance is achievable in a production environment.

3.3 PHYSICAL CONFIGURATION

An exploded view of the bandpass filter, F-1482()/GRC is shown in figure 3-17. The filter case, gear plates, rear cover, and front panel are aluminum. In this figure, the gear train cavity is observed, and it is noted that the front panel contains the metering circuitry, tuning knobs, and frequency dials. Behind each tuning knob is the associated gear train which translates the rotatory motion of the knob into the linear force necessary to adjust the variable capacitors to cause resonator resonance at the desired tune frequency. The circuit card assembly visible in the figure contains the phase discriminator. Immediately above the phase discriminator card is an opening through which hard wires carry the dc signal from the power discriminator up to the switch and meter located on the front panel.

Figure 3-18 shows the rear of the bandpass filter with the rear cover removed. The output connector and output resonator are on the left. Ground connections of each resonator helix are visible. The input coupling inductor, L7, is visible in the right (input) resonator compartment. To the right of this figure, the power discriminator printed circuit card and transceiver connector can be observed.

Maximum overall dimensions (including knobs, connectors, and mounting flanges) of the bandpass filter are 2.5 inches wide, 9.3 inches high, and 9.8 inches deep. The weight is approximately 6 pounds. An outline drawing of the bandpass filter is shown in figure 3-19.

Figure 3-20 shows the 5-channel combining network. This is a view into the interior of the coupler from the bottom, prior to foaming the assembly. Five 16.5-inch long connecting coaxial cables and the matching network are visible. Note all connections are soldered to reduce intermodulation distortion to the lowest possible level. The metal jacketed coaxial lines have sleeving installed over the outer conductors. This sleeving used is to prevent possible pressure contacts from occurring during the foaming operation. Foaming of this assembly ensures a rugged assembly capable of withstanding vibration and shock levels experienced during field transport by military vehicles. Since this assembly consists of highly reliable passive circuitry, maintainability is not sacrificed by foaming.

Figure 3-21 shows the 2-channel combining network. It is similar to the 5-channel network except it has two connecting coaxial cables.

Maximum overall dimensions of the 2-channel multiplexer are 7.4 inches wide, 11.1 inches high, and 12.3 inches deep. The maximum weight 17 pounds. An outline drawing of the 2-channel multiplexer is shown in figure 3-22.

Figure 3-23 is an outline drawing of the 5-channel multiplexer. Maximum overall dimensions are: 15.0 inches wide, 11.1 inches high, and 12.3 inches deep. The maximum weight is 37 pounds.

3.4 SCHEMATICS AND TUNING PROCEDURE

Schematics of the F-1482() GRC Bandpass Filter including the power discriminator and the phasing discriminator are shown in figure 3-24, 3-25, and 3-26.

Schematics of the 2-channel and 5-channel couplers are shown in figures 3-27 and 3-28.

Table 3-1 gives a step-by-step tuning procedure for the multiplexers.

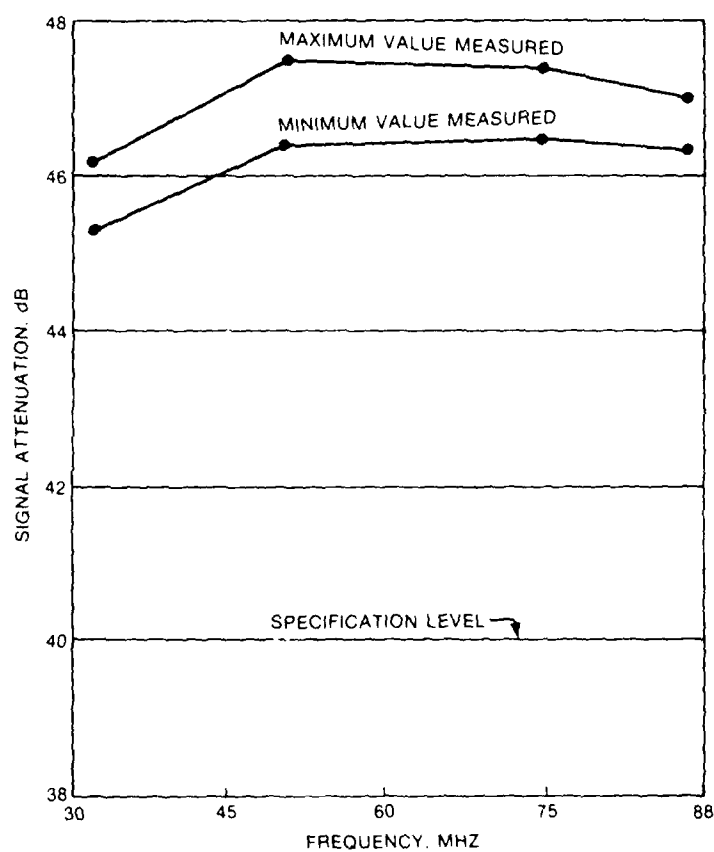


Figure 3-14. Measured Transceiver Port to Transceiver Port Attenuation.

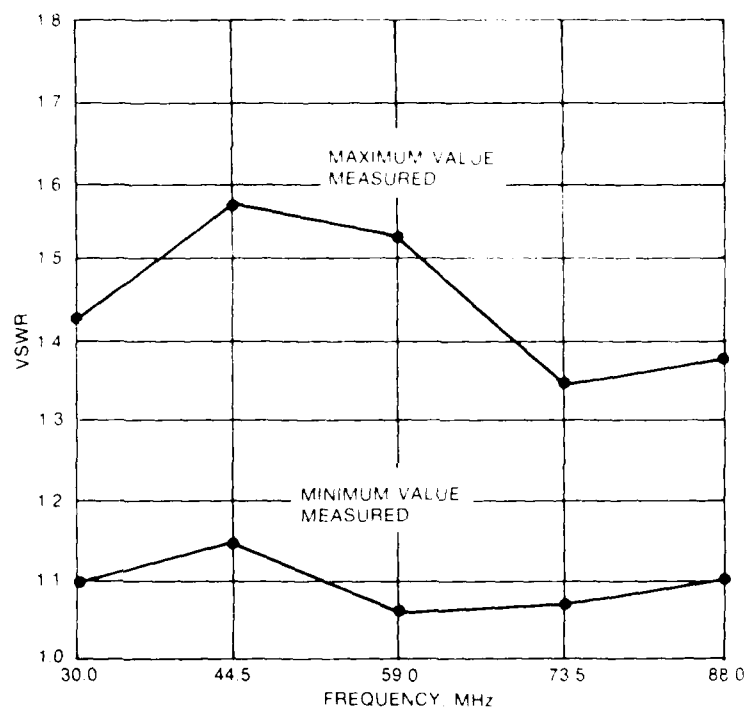


Figure 3-15. Measured VSWR at Transceiver Input.

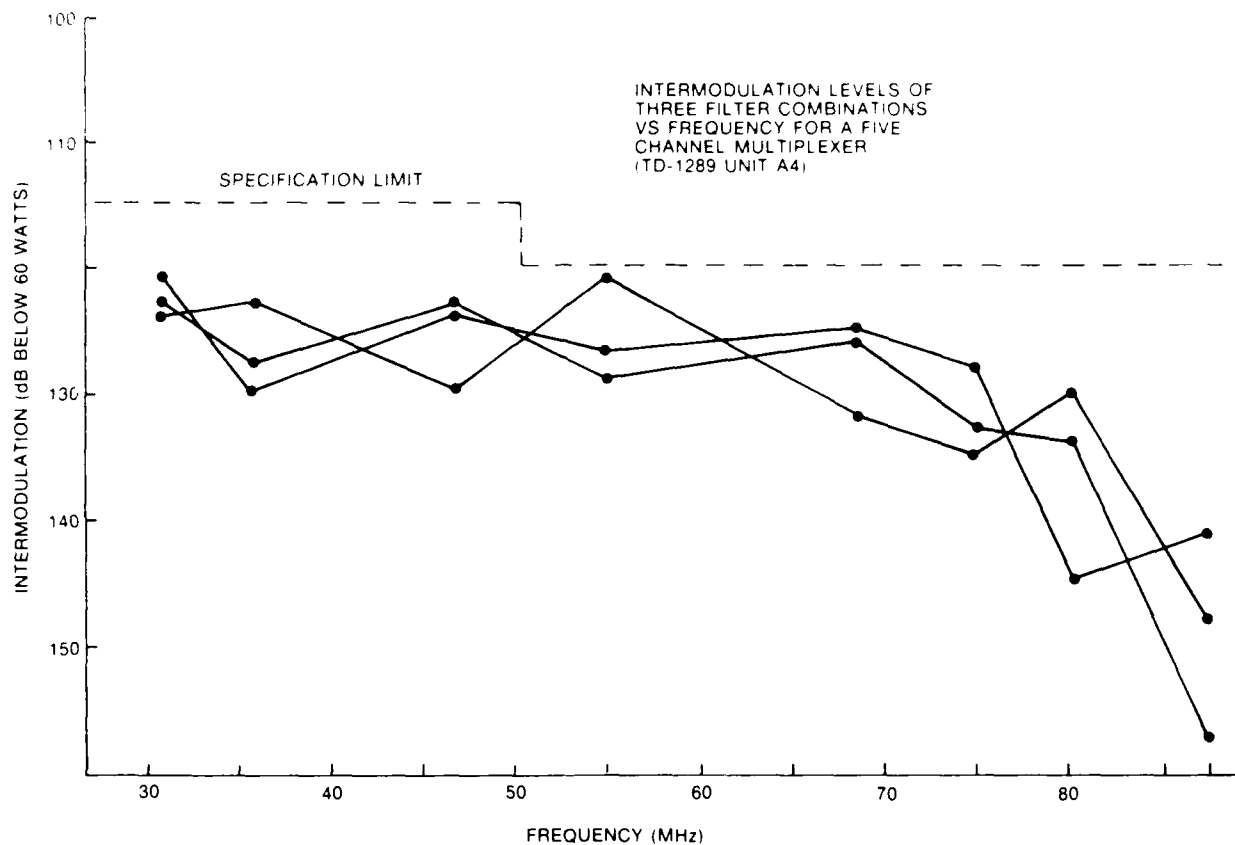


Figure 3-16. Intermodulation Levels of Three Filter Combinations vs Frequency for a 5-Channel Multiplexer With Improved Variable Capacitors (TD-1289())(V)1/GRC Unit 4A).



Figure 3-17. Bandpass Filter, Exploded View (F-1482()/GRC).



Figure 3-18. Bandpass Filter, Rear View (F-1482()/GRC).

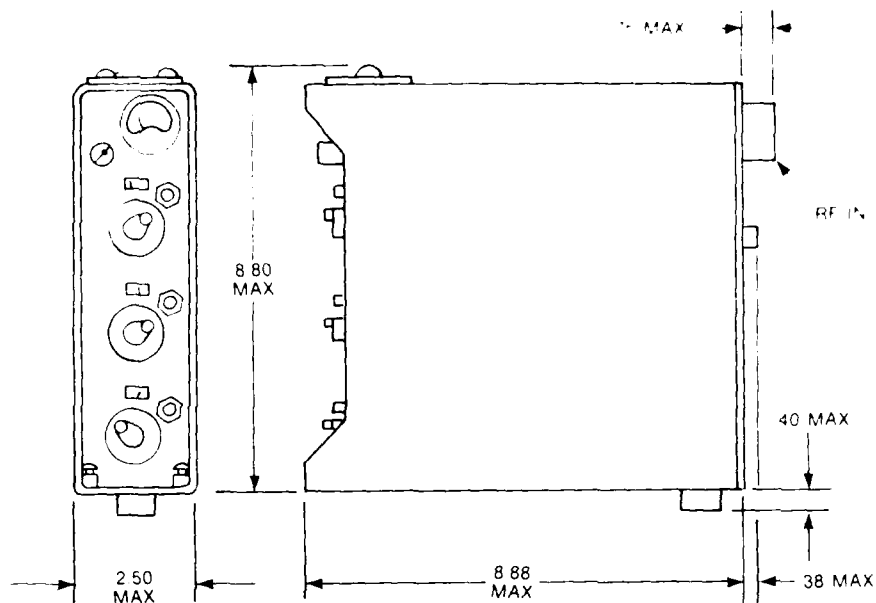


Figure 3-19. Outline Drawing, Bandpass Filter (F-1182() GRC).

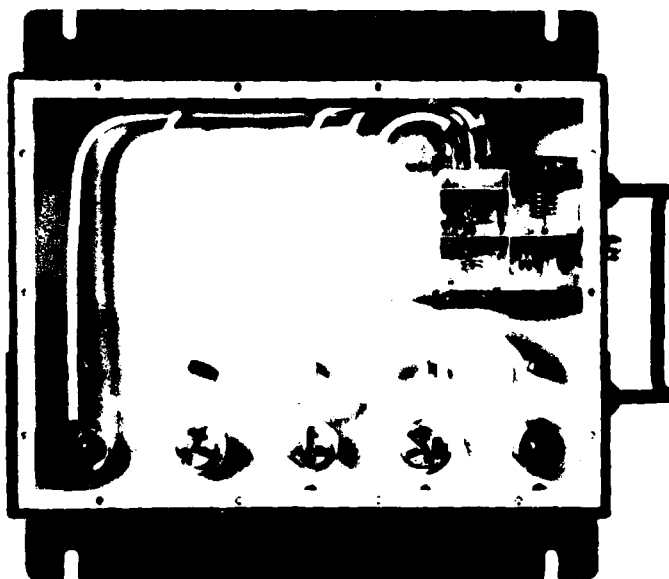


Figure 3-20. 5-Channel Coupler, Interior View (CU-2267() GRC).

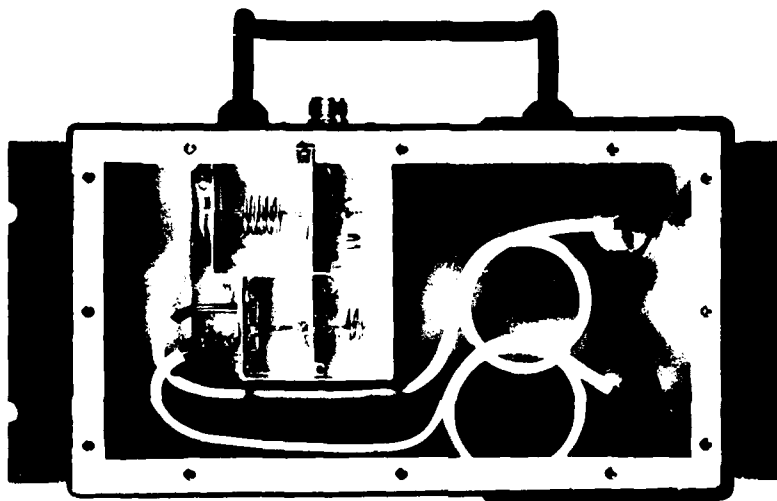


Figure 3-21. 2-Channel Coupler, Interior View (CU-2266() GRC).

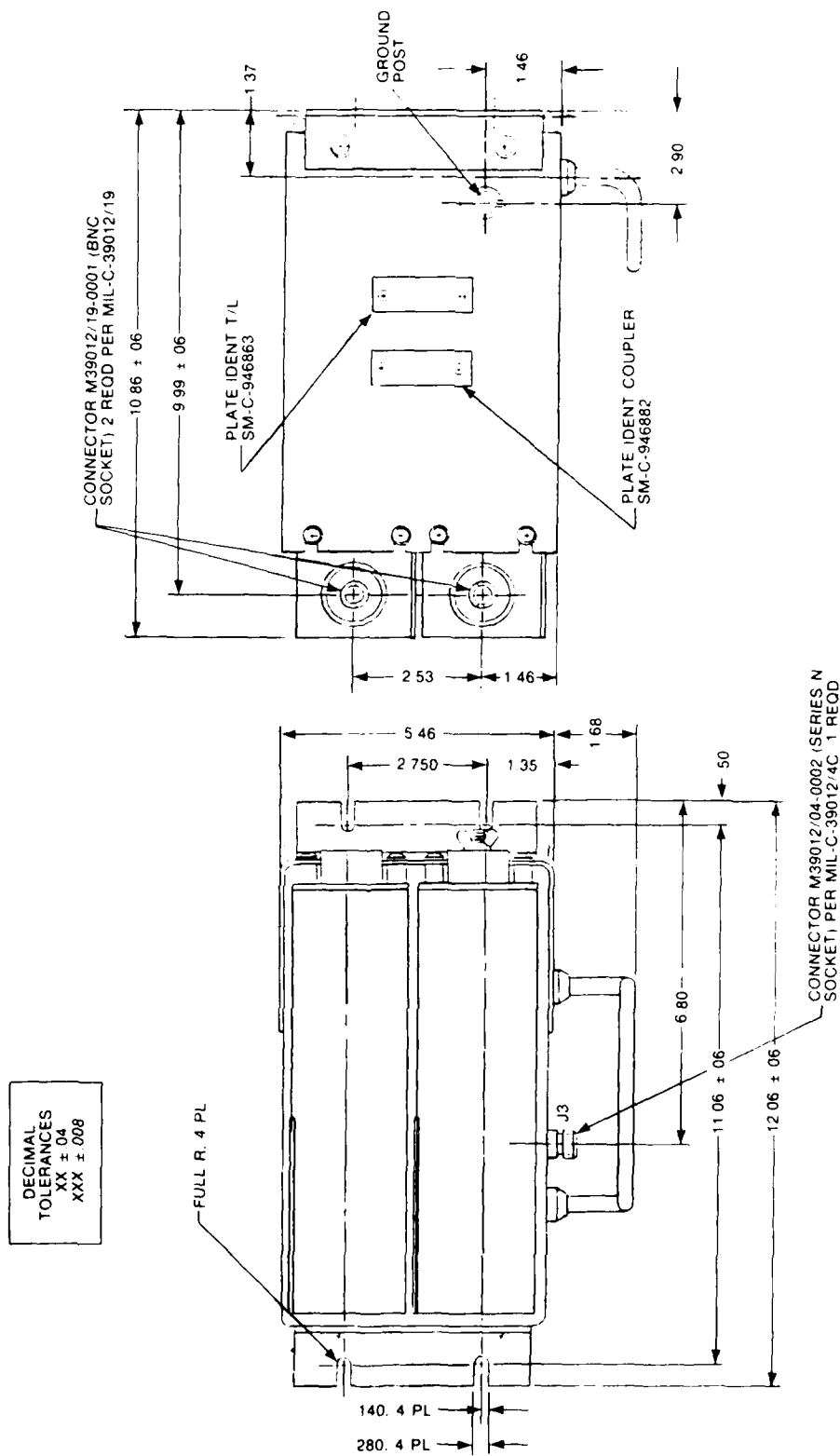


Figure 3-22. Outline Drawing, 2-Channel Multiplexer (TD-128S() GRC).

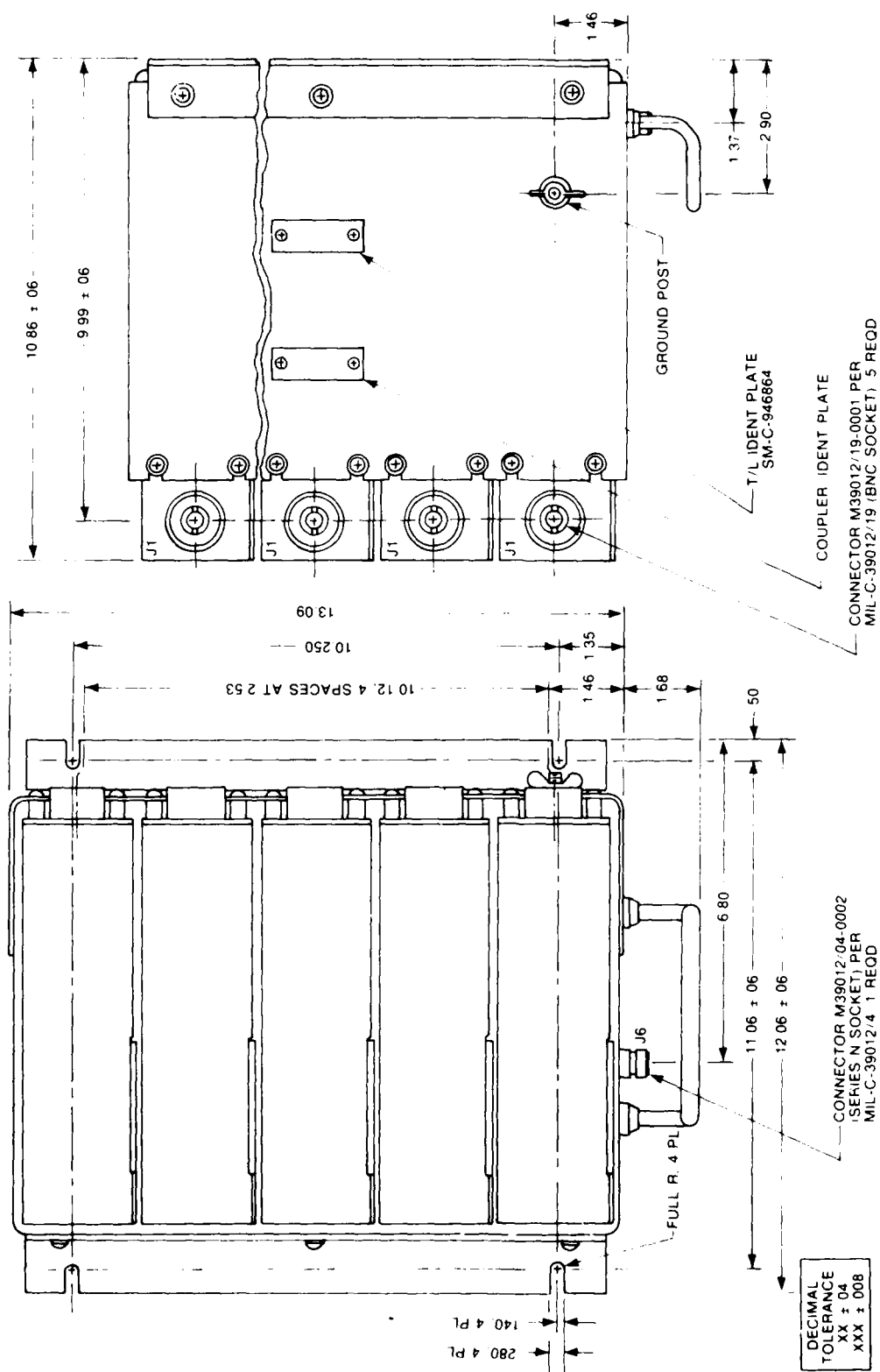


Figure 3-23. Outline Drawing, 5-Channel Multiplexer (TD-1289) (V1 GRC).

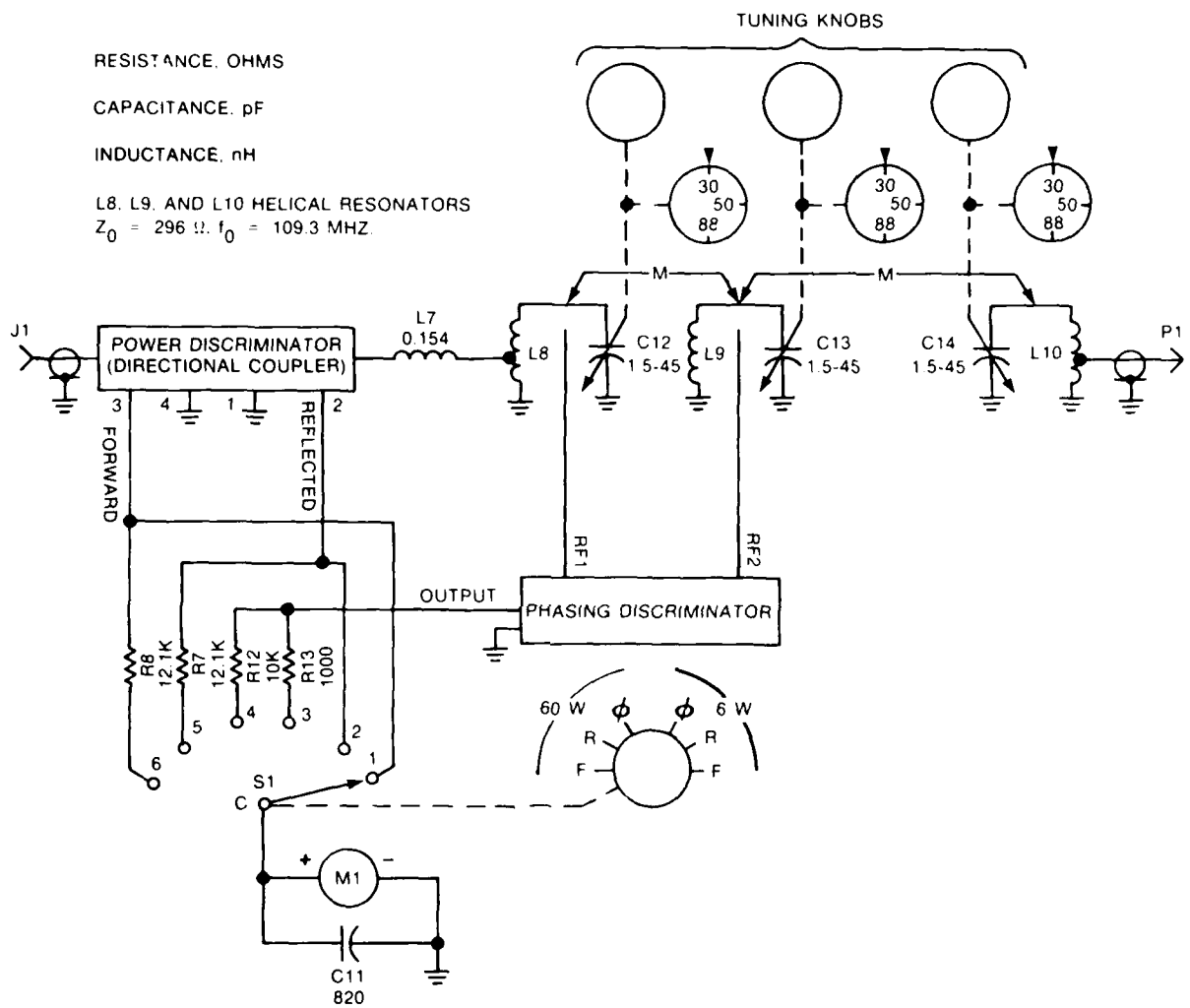


Figure 3-24. Schematic, Bandpass Filter (F-1482) /GRC).

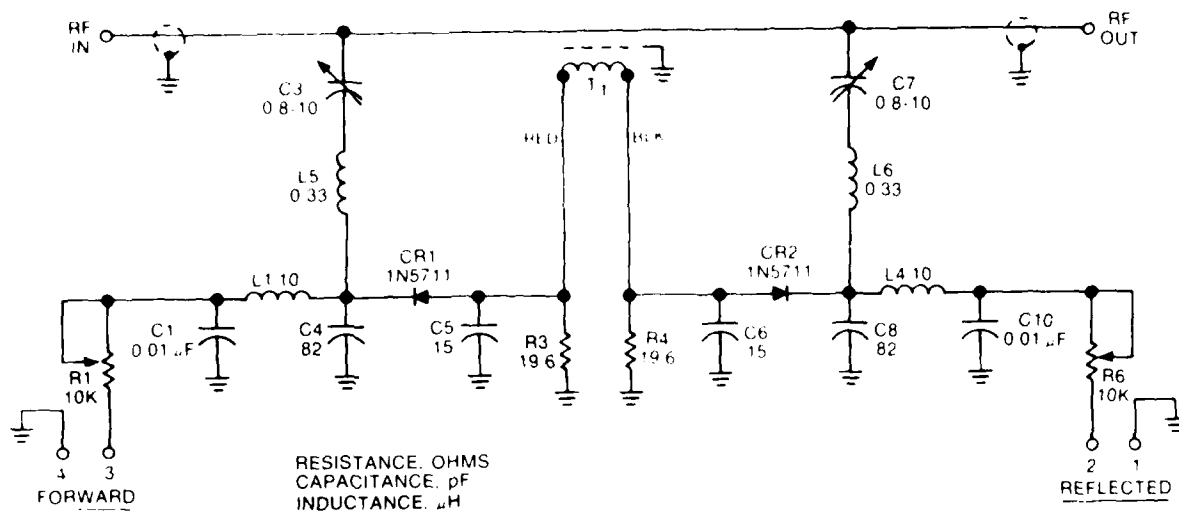


Figure 3-25. Schematic, Power Discriminator (Directional Coupler).

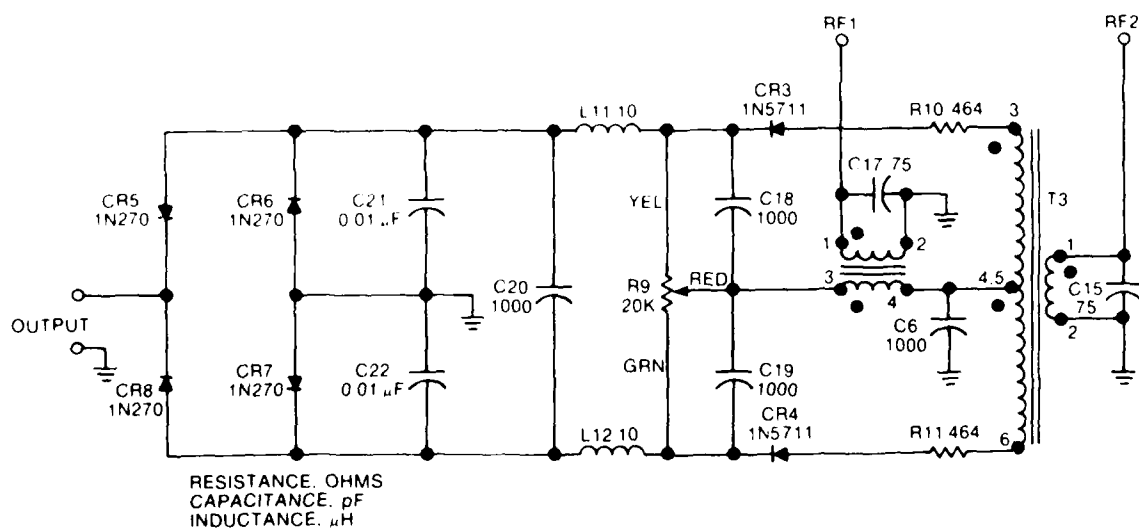


Figure 3-26. Schematic, Phasing Discriminator.

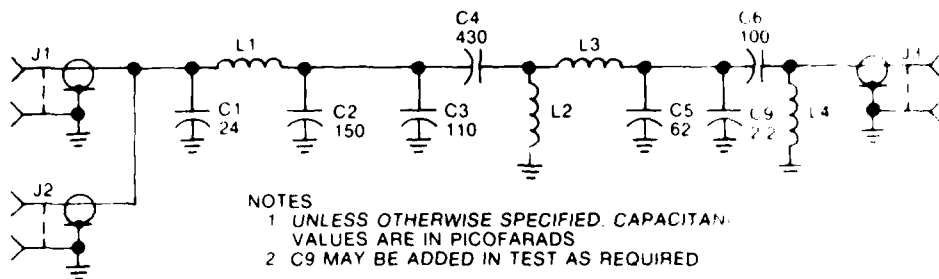


Figure 3-27. Schematic, 2-Channel Coupler (CU-2266) / GRC).

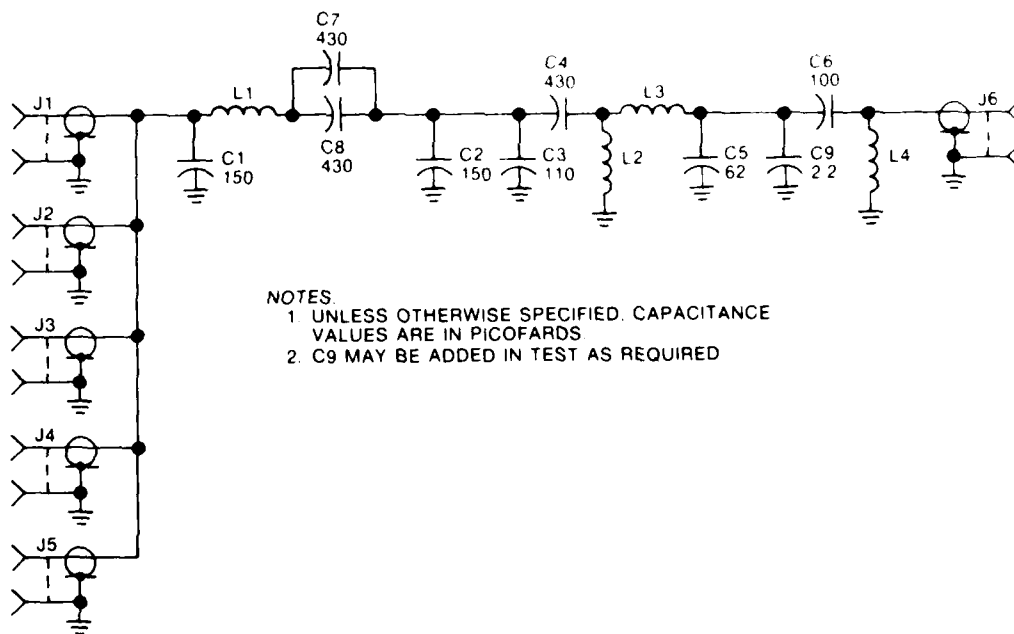


Figure 3-28. Schematic, 5-Channel Coupler (CU-2267) / GRC).

Table 3-1. Tuning Procedure for VHF Multiplexer.

- I. Prior to Tuning, Check the Following Conditions:
 1. No other filters are tuned to, or within 5% of the frequency about to be used.
 2. Rf power input to each bandpass filter will not exceed a nominal 60 watts.
 3. The antenna connector of the coupler must be connected to a 50-ohm broadband antenna or a 50-ohm load.
- II. Coarse Tuning before applying rf power:
 1. Unlock tuning knobs A, B, and C by turning lock knobs counterclockwise.
 2. Using tuning knobs A, B, and C, set the desired frequency in the center of the dial windows.
 3. Set the meter function switch to the 60 watt (60W) reflected power (R) position.
- III. Rf Tuning with rf power applied:

To avoid equipment damage, complete rf tuning steps 1 thru 5 within approximately 1 minute.

 1. Key the transceiver to apply rf power.
 2. Adjust tuning knob A for minimum reflected power as indicated by a minimum reading on meter. Adjust tuning knob B, and then tuning knob C, for a minimum reflected power.
 3. Set the meter function switch to 60 watt (60W) phase (Φ) position. Adjust tuning knob B for zero phase error.

Note

Zero phase error will be indicated by zero reading on the meter with a very sharp up-scale deflection on either side of the zero point.

4. Return the meter function switch to the 60W-R position. Readjust tuning knobs A and C for minimum reflected power.
5. Repeat steps 3 and 4 until the lowest reflected power and zero phase error are attained.
6. Set the meter function switch to 6 watt (6W) reflected power (R) position. Readjust tuning knobs A and C for minimum reflected power.
7. Set the meter function switch to the 6 watt (6W) phase (Φ) position. Adjust tuning knob B for zero phase error.
8. Repeat steps 6 and 7 until the lowest reflected power and zero phase error are attained. Tuning is complete.
9. Lock the three tuning knobs with a finger-tight rotation of the lock knob. Do not use tools.

Section 4

Literature Cited

1. S.B. Cohn, "Dissipation Loss in Multiple-Coupled-Resonator Filters," Proceedings of the IRE, pp 1342-1348 (August 1959).
2. George L. Matthaei, Leo Young, E.M.T. Jones, "Microwave Filters, Impedance-Matching Networks, and Coupling Structures," McGraw-Hill, 1964, p 100.
3. Reference Data for Radio Engineers, 4th Ed., pp 1090-1097, I.T.T., N.Y., 1956.
4. H.L. Landt, "Design of Minimum Loss Filters Using Any Number of Resonators," WP-4738, January 23, 1967, Collins Radio Company, Cedar Rapids, Iowa.
5. A.I. Zverev, "Handbook of Filter Synthesis" Wiley, New York, 1967.
6. R.M. Fano, "Theoretical Limitations on the Broadband Matching of Arbitrary Impedances," J. Franklin Inst, Vol 249, pp 57-83 and 139-154 (January and February 1950).
7. G.L. Matthaei, "Synthesis of Tchebycheff Impedance-Matching Networks, Filters, and Interstages," IRE Trans PGCT 3, pp 162-172 (September 1956).

101	Defense Technical Info Ctr ATTN: DTIC-TCA Cameron Station (Bldg 5) Alexandria, VA 22314	215	Naval Telecommunications Cmd Tech Library, Code 911 4401 Massachusetts Avenue, NW Washington, DC 20390
*012		001	
102	Director National Security Agency ATTN: TDL Fort George G. Meade, MD 20755	217	Naval Air Systems Comd Code: Air-5332 Washington, DC 20360
001		004	
103	Code R123, Tech Library DCA Defense Comm Engrg Ctr 1860 Wiehle Ave Reston, VA 22090	219	Dr. T.G. Berlincourt Ofc of Naval Research (Code 420) 800 N. Quincy Street Arlington, VA 22217
001		001	
104	Defense Comm Agency Tech Library Ctr Code 205 (P.A. Tolovi) Washington, DC 20305	300	AUL LSE 64-285 Maxwell AFB, AL 36112
002		001	
200	Office of Naval Research Code 427 Arlington, VA 22217	301	Rome Air Development Ctr ATTN: Documents Library (TSLD) Griffiss AFB, NY 13441
001		001	
205	Commanding Officer Naval Research Lab ATTN: Code 2627 Washington, DC 20375	302	USAFETAC (CBTL) ATTN: Librarian Stop 825 Scott AFB, IL 62225
001		001	
206	Commander Naval Oceans Systems Ctr ATTN: Library San Diego, CA 92152	304	Air Force Geophysics Lab L.G. Hanscom AFB ATTN: LIR Bedford, MA 01730
001		001	
207	CDR, Naval Surface Weapons Ctr White Oak Lab ATTN: Library, Code WX-21 Silver Springs, MD 20910	307	AFGL SU1.1. S-29 HAFB, MA 01731
001		001	
210	Commandant, Marine Corps HQ, US Marine Corps ATTN: Code LMC Washington, DC 20380	312	HQ, AFEWC ATTN: EST San Antonio, TX 78243
002		002	
211	HQ, US Marine Corps ATTN: Code INTS Washington, DC 20380	314	HQ, Air Force Systems Cmd ATTN: DLWA Mr. P. Sandler Andrews AFB Washington, DC 20331
001		001	
212	Command, Control & Comm Div Development Ctr Marine Corps Development & Education Command Quantico, VA 22134	403	Commander, MICOM Redstone Scientific Info Center ATTN: Chief, Document Section Redstone Arsenal, AL 35809
001		002	

*Reduce to 2 copies if report bears a limited distribution statement.

404	Commander, MICOM ATTN: DRSMI-RE (Mr. Pittman)	455	Commandant US Army Signal School
001	Redstone Arsenal, AL 35809	ATTN: ATZH-CD	
406	Commandant US Army Aviation Ctr	001	Fort Gordon, GA 30905
	ATTN: ATZQ-CD-MA	456	Commandant
001	Fort Rucker, AL 36362	US Army Infantry School	
408	Commandant US Army Military Police School	ATTN: ATSH-CD-MS-E	
	ATTN: ATZN-CDM-CE	001	Fort Benning, GA 31905
003	Fort McClellan, AL 36205	462	CDR, ARRCOM
417	Commander US Army Intelligence Ctr & School	ATTN: Systems Analysis Ofc,	
	ATTN: ATSI-CD-MD	DRSAR-PE	
003	Fort Huachuca, AZ 85613	001	Rock Island, IL 61299
418	Commander HQ Fort Huachuca	470	Dir of Combat Developments
	ATTN: Technical Ref Div	US Army Armor Ctr	
001	Fort Huachuca, AZ 85613	ATTN: ATZK-CD-MS	
419	Commander US Army Elet Proving Ground	002	Fort Knox, KY 40121
	ATTN: STEEP-MT	474	Commander
001	Fort Huachuca, AZ 85613	US Army Test & Evaluation Cmd	
422	Commander US Army Yuma Proving Ground	ATTN: DRSTE-CT-C	
	ATTN: STEYP-MTD (Tech Library)	001	Aberdeen Proving Ground, MD
001	Yuma, AZ 85364	21005	
432	Dir, US Army Air Mobility R&D Lab	475	CDR, Harry Diamond Lab
	ATTN: T. Gossett, Bldg 207-5	ATTN: Library	
	NASA AMES Research Ctr	2800 Powder Mill Road	
001	Moffett Field, CA 94035	001	Adelphi, MD 20783
436	HQDA (DAMO-TCE)	477	Director
002	Washington, DC 20310	US Army Ballistic Research Lab	
437	Deputy for Science & Tech	ATTN: DRNBR-LB	
	Office, Asst Sec Army (R&D)	001	Aberdeen Proving Ground, MD
002	Washington, DC 20310	21005	
438	HQDQ (DAMA-ARZ-D. Dr. F. D.	479	Director
	Verderme)	US Army Human Engineering Lab	
001	Washington, DC 20310	001	Aberdeen Proving Ground, MD
		21005	
		482	Director
		US Materiel Systems Analysis	
		Activity	
		ATTN: DRXSY-T	
		001	Aberdeen Proving Ground, MD
		21005	

483	Director US Army Materiel Systems Analysis Activity ATTN: DRNSY-MP	518	TRI-TAC Office ATTN: TT-DA
001	Aberdeen Proving Ground, MD 21005	001	Fort Monmouth, NJ 07703
503	Director US Army Engr Waterways Exper Station ATTN: Research Ctr Library	519	CDR, US Army Avionics Lab ARRADCOM ATTN: DAVAA-D
002	Vicksburg, MS 39108	001	Fort Monmouth, NJ 07703
504	Chief, CERCOM Aviation Elet Ofc ATTN: DRSEL-MME-LAF(2)	529	CDR, US Army Research Ofc ATTN: Dr. Horst Wittmann PO Box 12211
001	St. Louis, MO 63166	001	Research Triangle Park, NC 27709
507	CDR, AVRADCOM ATTN: DRSAY-E PO Box 209	531	CDR, US Army Research Ofc ATTN: DRNRO-IP PO Box 12211
001	St. Louis, MO 63166	002	Research Triangle Park, NC 27709
512	Commander ARRADCOM ATTN: DRDAR-1CN-S (Bldg 95)	533	Commandant US Army Inst for Military Asst ATTN: ATSU-CTD-MO
001	Dover, NJ 07801	002	Fort Bragg, NC 28307
513	Commander ARRADCOM ATTN: DRDAR-TSS, #59	536	Commander US Army Arctic Test Ctr ATTN: STEAC-TD-MH
001	Dover, NJ 07801	002	APO Seattle 98733
514	Director Joint Comm Ofc (TRI-TAC) ATTN: TT-AD (Tech Doc Cntr)	542	Commandant USAFAS ATTN: ATSF-CD-DE
001	Fort Monmouth, NJ 07703	001	Fort Sill, OK 73503
515	PM, FIREFINDER REMBASS ATTN: DRC PM-FER BLDG 2539	554	Commandant US Army Air Defense School ATTN: ATSA-CD-MS-C
001	Fort Monmouth, NJ 07703	001	Fort Bliss, TX 79916
516	Project Manager, NAVCON ATTN: DRC PM-NC-TM Bldg 2539	563	Commander, DARCOM ATTN: DRCDE 5001 Eisenhower Ave
001	Fort Monmouth, NJ 07703	001	Alexandria, VA 22333
517	Commander US Army Satellite Comm Agey ATTN: DRC PM-SC-3	565	CDR, US Army Signals Warfare Lab ATTN: DELSW-SO Vint Hill Farms Station
002	Fort Monmouth, NJ 07703	002	Warrenton, VA 22186

566	CDR, US Army Signals Warfare Lab ATTN: DELSW-AQ Vint Hill Farms Station 001 Warrenton, VA 22186	604	Chief Ofc of Missile Electronic Warfare Electronic Warfare Lab ERADCOM 001 White Sands Missile Range NM 88002
567	Commandant US Army Engineer School ATTN: ATZA-TDL 002 Fort Belvoir, VA 22060	606	Chief Intel Materiel Dev & Support Office Electronic Warfare Lab ERADCOM 001 Fort Meade, MD 20755
569	Commander US Army Engineer Topographic Labs ATTN: ETL-TD-EA 001 Fort Belvoir, VA 22060	608	Commander US Army Ballistic Rsch Lab ARRAIDCOM ATTN: DRDAR-TSB-S (STINFO) 001 Aberdeen Proving Ground, MD 21005
572	Commander US Army Logistics Ctr ATTN: ATCL-MC 002 Fort Lee, VA 22801	612	CDR, ERADCOM ATTN: DRDEL-CT 2800 Powder Mill Road 002 Adelphi, MD 20783
575	Commander TRADOC ATTN: ATDOC-TA 001 Fort Monroe, VA 23651	619	CDR, ERADCOM ATTN: DRDEL-PA 2800 Powder Mill Road 001 Adelphi, MD 20783
577	Commander US Army Training & Doctrine Cmd ATTN: ATCD-TM 001 Fort Monroe, VA 23651	622	HQ, Harry Diamond Lab ATTN: DELHD-TD (Dr. W W. Carter) 2800 Powder Mill Road 001 Adelphi, MD 20783
578	CDR, US Army Garrison Vint Hill Farms Station ATTN: LAVAAF 001 Warrenton, VA 22186	680	Commander ERADCOM Fort Monmouth, NJ 07703 1 DELEW-D 1 DELCS-D 1 DELET-D 1 DELSD-L 1 DELSD-D *2 DELSD-L-S
579	Proj Mgr, Control & Analysis Ctrs Vint Hill Farms Station 001 Warrenton, VA 22186		
602	CDR, Night Vision & Electro-Optics Laboratory ERADCOM ATTN: DELNV-D 001 Fort Belvoir, VA 22060		
603	CDR, Atmospheric Sciences Lab ERADCOM ATTN: DELAS-SY-S 001 White Sands Missile Range, NM 88002		

*Furnish only unclassified reports.

681 Commander, CECOM
Fort Monmouth, NJ 07703

1 DRSEL-PPA-S
1 DRSEL-COM-D
1 DRSEL-TCS-B
1 DRSEL-PL-ST
1 DRSEL-MA-MP
1 DRSEL-LE-RI
1 DRSEL-PA
1 DRSEL-LE-C
3 DRSEL-COM
25 DRSEL-COM-RN

701 MIT-Lincoln Lab
ATTN: Library (Rm A-082)
PO Box 73
002 Lexington, MA 02173

703 NASA Scientific & Tech Info Facility
Baltimore Washington Intl Airport
001 PO Box 8757, MD 21240

704 National Bureau of Standards
Bldg 225, RM A-331
ATTN: Mr. Leedy
001 Washington, DC 20231

706 Advisory Group on Electron Devices
ATTN: Secy, Working Grp D (Lasers)
201 Varick Street
002 New York, NY 10014

707 TACTEC
Battelle Memorial Inst
505 King Ave
001 Columbus, OH 43201

709 Plstics Tech Eval Ctr
Picatinny Arsenal, Bldg 176
ATTN: Mr. A.M. Anzalone
001 Dover, NJ 07801

710 Ketron, Inc.
1400 Wilson Blvd, Architect Bldg
002 Arlington, VA 22209

712 R. C. Hansen, Inc.
PO Box 215
001 Tarzana, CA 91356

714 Dynallectron Corp
GIDEP Engineering & Support
Department
PO Box 398
001 Norco, CA 91760

DATE
FILMED
8-8